Recent Advances in the Measurement of Strongly Radiating, Turbulent Reacting Flows

G. J. Nathan[a,c,*], P. A. M. Kalt[a,c], Z. T. Alwahabi[b,c], B. B. Dally[a,c], P. R. Medwell[a,c], Q. N. Chan[b,c]

[a] *School of Mechanical Engineering, The University of Adelaide, S.A. 5005 Australia*
[b] *School of Chemical Engineering, The University of Adelaide, S.A. 5005 Australia*
[c] *Centre for Energy Technology, The University of Adelaide, S.A. 5005 Australia*

Abstract

Recent advances in diagnostic methods are providing new capacity for detailed measurement of turbulent, reacting flows that are strongly radiating. Radiation becomes increasingly significant in flames containing soot and/or fine particles, and also increases with physical size, therefore many flames of practical significance are strongly radiating. Under these conditions, the coupling between the turbulence, chemistry and radiative heat transfer processes are also significant, making it necessary to obtain simultaneous measurement of controlling parameters. However, these environments are also particularly challenging for laser-based measurements, since soot and other particles cause additional interferences to the signal and also increased attenuation of the beam. The paper reviews the influence of physical scale and resolution on reacting systems and measurement approaches. It then reviews the recent advances in techniques to measure temperature, mixture fraction, soot volume fraction, velocity, particle number density and the scattered, absorbed

*Corresponding author. Fax: +61 8 8303 4367
Email address: graham.nathan@adelaide.edu.au (G. J. Nathan)

and transmitted components of radiation propagation through particle laden systems and the further influences of facility size. Finally it also considers remaining challenges to diagnostic techniques under such conditions.
Keywords: Radiation heat transfer, Laser Diagnostics, Soot, Turbulent reacting flows

---

1. Introduction

Radiation is the dominant mode of heat transfer in most practical high temperature thermal processes, owing to the fourth power dependence of radiant heat transfer on the temperature differential. For this reason, considerable effort has been expended to understand and predict radiation heat transfer and great progress has been made. It is well established that the turbulent processes are directly coupled to the radiation heat transfer in reacting flows, and these influences can be very significant. Substantial progress has been made in capacity to account for these coupling processes, but mostly under conditions where scattering can be ignored [1]. However, scattering cannot be ignored in the presence of soot and/or particulate fuels. Furthermore, the presence of particles such as soot adds greatly to the complexity of reacting flows, and hence further to the computational requirements of simulations since it increases the strength of the coupling between turbulence, radiation and reactions. Even without the presence of particles, the development of reliable models requires detailed, well-resolved and simultaneous measurements of the key controlling parameters. To meet this need, laser diagnostics have been developed to provide unrivalled edge over intrusive probes in terms of spatial and temporal resolution and species selectivity [2].

However, despite their substantial contribution to combustion science, many of these laser diagnostic tools are limited to application in environments that avoid the presence of soot — along with most of the other complexities of practical systems, which include large physical scale, multiple phases, multi-component fuels, inorganic species, secondary turbulent motions and high pressure. Nevertheless, a number of laser-based diagnostic methods are emerging which promise to open new windows into these complex processes on which radiant heat transfer depends. The aim of the paper is to review these methods.

The need for improved capacity to understand and predict radiative heat transfer in and from flames is driven by the challenge to supply ever-cleaner energy. Radiation is typically the dominant mode of heat transfer in flames containing soot or particulate fuels, so influences both energy efficiency and pollutant formation, through temperature [3]. The need to optimise combustion systems is increasing, despite an increase in the use of renewable energy. The Intergovernmental Panel on Climate Change predicts a growth in the utilization of all fuels to 2030 by 52%. Also, while a significant drop in world-wide coal utilization for power generation from 23.9 to 17% over the period to 2030, owing to the switch to natural gas fired integrated gas turbine combined cycles (IGCC), the absolute utilization of coal is expected to increase by about 1% [4]. It should also be noted that, while pyrolysis and gasification may reduce the proportion of combustion, this does not obviate the need for capacity to provide detailed measurements. The use of gasification and pyrolysis offers some advantages in allowing the ash to be retained in the char. However, gasifiers and pyrolysis systems are typically even more

complex to investigate in detail than combustion systems, operating under very dense particle loadings, where optical access is even more difficult. Producer gas is also typically of relatively high sooting propensity. Furthermore, new technologies are emerging such as solar gasification [5, 6] in which the need to obtain detailed understanding and modelling capacity of radiation in complex media is paramount for design optimisation. Hence there is an ever-growing need to overcome the challenges for spatially and temporally resolved measurements of the parameters controlling radiation heat transfer in complex environments.

Computational capability has advanced to the stage where the direct numerical simulation (DNS) of turbulent reacting systems is now possible [7]. Nevertheless, DNS of turbulent reacting systems is unlikely to become a tool of choice for predictive purposes as it is limited to very small physical domains, relatively simple flows and relatively simple chemistry [8]. This is especially true in the investigation of radiation heat transfer in realistic systems [1]. Instead DNS is used to provide complex and dependent correlations for combustion models: essentially small scale numerical experiments. Likewise, the understanding of chemical kinetics has advanced to the extent where reliable reduced mechanisms are now available for a significant number of hydrocarbon fuels [9] and surrogate gasoline fuels [10]. Nevertheless a substantial challenge remains to expand this research to the stage where such schemes are available for many practical fuels [9, 10]. These issues mean that the development of models for practical combustion systems, necessarily with a limited range of validity, will continue to rely on experimental data for the foreseeable future for model development and validation. Hence the mea-

surement of temperature, along with mixture fraction and particle volume fraction, on which emissivity depends, are critical to determining radiation. Furthermore, because radiation propagates along rays, there is a significant advantage in planar measurements, from which line-of-sight data can be obtained. Simultaneous planar measurement of these parameters is therefore highly desirable.

The key challenges to the extension of laser diagnostics to resolve the parameters on which into radiation depends in turbulent reacting flows involving soot, particulate fuels and larger physical scale are:

- **Increased background interference**: Optical interference increases with the presence of any particles, which radiate incandescently and/or scatter laser signal. The natural background radiation from a flame also increases with the size of the flame and the use of furnace walls.

- **Optical attenuation**: The attenuation of both the incoming laser beam and the outgoing laser-generated signal (termed "signal trapping" increases with the introduction of particles and/or the size of a flame.

- **Reduction in spatial fidelity**: Both beam steering due to density gradients, and optical diffraction due to particles, lead to an increase in the uncertainty in spatial location.

- **Increased number of parameters to measure**: The number of parameters to measure increases dramatically with the use of particulate, multi-component fuels that contain fuel impurities (*i.e.* inorganic components). These include particle size, shape, number density, composition and temperature.

- **Reduced optical access**: Investigations of large scale and/or pressured systems entail reduced optical access into the flame and may require optical probes to be inserted into the flame to achieve sufficient optical penetration.

Given these challenges, the aim of the present paper is to review progress and ongoing challenges in present ability to perform spatially and temporally resolved measurements of increasing relevance to practical reacting flows. Particular emphasis is placed on the use of planar measurement techniques, since these offer many advantages in the understanding of turbulent reacting flows and also allow for ray tracing of radiation. Despite their practical significance, the investigation of pressurised combustion and the measurement of inorganic species are outside the scope of the present review.

2. Measurement requirements

The requirements for measurements to be suitable for the development and validation of detailed models in turbulent reacting flows have been reviewed previously [11]. Such measurements should:

- employ well defined initial and boundary conditions,
- measure multiple parameters simultaneously,
- measure multiple dimensions — planar or 3D,
- resolve spatial and temporal gradients of interest.

Even apparently small changes to the in-flow conditions, such as differences in a boundary layer profile, can influence a flow or flame as they

propagate into the far field [12]. This issue has driven the need for well-characterised in-flow and boundary conditions for flames to be suitable for model development and validation — a process well demonstrated by the International Turbulent Non-premixed Flame Workshop [13].

The challenge to achieve well-resolved and simultaneous measurement of key controlling parameters in turbulent systems has been driving research for many years [11]. This need arises because of the unsteady and non-linear relationship between the controlling parameters of even isothermal turbulent flows, which increase with reactions. Considerable effort has thus been invested to define and resolve the smallest scale of turbulent flows, the Kolmogorov scale, λ_K, and of turbulent mixing, the Bachelor scale, λ_B, along with scalar gradients and the scalar dissipation [14–16]. The challenge to resolve scalar dissipation in reacting flows has only recently been met with the breakthrough work of Wang *et al.* [17]. Such methods could, in principle, be extended to larger scale, which would be valuable for systems such as lean pre-mixed gas turbines, where localised extinction under high strain is a particularly important issue.

The controlling parameters for turbulent flows transporting reacting particles are strongly coupled, providing increased need for simultaneous measurements. A notable example is the coupled dependence of soot volume fraction on temperature [18, 19]. Both the formation and oxidation of soot depend upon fuel type, mixture fraction, ξ (the local mass fraction of species originating from the fuel stream), temperature, T [20], and on the residence time (and hence on strain rate) in the reaction zone [21]. At the same time, T also depends on soot concentration, which dominates radiant heat trans-

fer, and on turbulent mixing through fluid properties. Likewise, the rates of heating and reaction of fuel particles depends on the local temperature, and the volatile gases and energy they release influence T. Also, the processes of droplet evaporation and gasification or devolatilisation are also endothermic.

The many large-scale coherent motions inherent in turbulent systems make planar measurements desirable. Planar images permit the acquisition of spatially correlated measurements and the measurement of scalar gradients, which are useful both in scientific research and in the study practical combustion systems [22]. They also provide physical insight that is not possible with single point measurements.

3. Need for, and challenges to, measurements in large scale flames

Thermal processes become increasingly cost-effective and efficient with increased physical size. There is therefore an ongoing need to develop models that can be applied at ever-increasing scale. At the same time, model development and validation is expensive, and is inevitably undertaken predominantly at smaller scale where more detailed access is possible. This raises the challenge that flames of sufficiently different physical scale can exhibit quite different behaviour. This point is illustrated below by comparing four of the key dimensionless parameters that characterize some of the most important physical processes in a typical full-scale pulverized fuel flame and a geometrically similar model at $1/10^{\text{th}}$ scale. It is particularly the case with radiation heat transfer in the presence of soot and fine particles, where sufficiently large scale can result in the attenuation of radiation. These differences mean that reliable prediction of the processes on which radiation depends at

industrial-scale requires experimental data at comparable scale, and cannot rely solely on data at low Reynolds number and/or small physical scale. The optical thickness of a flame also increases with physical scale [1] and the radiative properties of fires become fundamentally different at sufficiently large scale [23].

Table 1 presents the key physical parameters of the burner and flame. Here d and U represent a reference diameter and bulk mean velocity characterising the burner. In practice all industrial burners are complex, with multiple streams of fuel and oxidizer, often containing swirl *etc.*. However, since the reference and model systems are geometrically similar, any single reference diameter can be used, so long as it is consistent. Likewise, the particles inevitably comprise a wide distribution, but provided that same relative size distribution is used, any reasonable reference size can be used. In principle it is possible to operate with reduced size particles, but in practice this is rarely done owing to the added cost and difficulty in reducing the size sufficiently to maintain similarity. The dimensionless parameters compared are the Reynolds Number, $Re = \rho U d/\mu$, the characteristic residence time (*e.g.* of a coal particle) in a flame, $\tau_{res} = L_F/U$, the ratio of flow speed to laminar flame speed, U/S_L and the Stokes Number, $Sk = \rho_p U d_p^2/18\mu L_t$, which describes the ratio of particle response time to a characteristic eddy time. Here L_t is the length scale of the large turbulent eddies, which also scale with L_F and the other symbols have their usual meanings.

From the data in Table 2 it is clearly not possible to select a velocity for the pilot-scale model that does not result in at least an order of magnitude change in at least two dimensionless parameters, and this list of dimension-

less groups is not intended to be exhaustive. Of course, the influence of many dimensionless parameters is typically asymptotic. For example, a change in Re will not have a large influence when it is sufficiently high to be in the fully turbulent regime. Hence, a pilot-scale program should be designed so dimensionless groups with the greatest influence are analogous to real conditions [24]. Without this, a smaller scale facility could operate in an entirely different regime (or mode) of behaviour. Nevertheless, some compromise is inevitable and model validation at the laboratory scale will not automatically result in reliable prediction at the industrial scale.

Further evidence of the influence of physical scale on performance of flames is found in the scaling assessment of Weber [25]. Figure 1 presents the NOx emissions measured from a series of geometrically similar burners each scaled by constant velocity scaling. It is evident that the emissions depend on physical scale, and that there is no simple way to scale from one flame to another.

The requirement for data at realistic physical scales is well known, and extensive measurements have been performed at pilot-scale, to contribute to model development and validation. An example of such a program in boiler flames is the extensive data sets from International Flame Research Foundation [26, 27]. Despite their value, such data were, for many years, typically limited to mean values of temperature and stable species, as obtained by suction probes, and to two-component velocity obtained by LDA. Pilot scale investigations assessing heat flux and total emissions have also played a vital role in technology development [27–29]. More recently, the extensive investigations by Sandia of larger scale pool fires have included single point

measurements of soot volume fraction [30] and temperature [31] using semi-intrusive laser diagnostics. These have provided significant new insights and demonstrate the benefits that are possible with further developments in laser diagnostic measurement capability. Nevertheless, such data are uncommon and there remains a significant need for reliable data in flames of significant scale for the development and validation of models of radiation heat transfer [1].

Turbulent mixing occurs at a wide range of scales. The smallest scale of turbulence is characterised by the Kolmogorov scale, λ_K, which can be estimated for a jet from the well-known relation of Antonia *et al.* [32] to be:

$$\lambda_K = LC_1 Re_L^{-0.75} \ . \tag{1}$$

Here L is the local width of the jet, which in turn scales with the nozzle diameter, d, while C_1 is a constant (for a non-reacting system), which for a cold jet is estimated to be 2.4. Hence the smallest scales of turbulence, λ_K are typically about the same at industrial scale as at the laboratory scale, while the largest scales of motions, *i.e.* L, are much greater at the industrial scale. The additional challenges for experimental techniques at a large physical scale result because chemical reactions occur at the molecular scale while the energy-containing turbulent eddies that typically control mixing, occur at the largest scale of the system. The separation between these turbulent scales increases with the physical size of the system. Hence pilot- or industrial-scale systems have a wide separation of scales, making computation of large turbulent systems difficult. For example at constant velocity and temperature

$$L/\lambda_K \propto (d_{full}/d_{mod})^{0.75} \ . \tag{2}$$

A similar ratio will apply for the Batchelor scale [14]. This means that the difficulty of simultaneously resolving both large and small scales increases with the scale of the facility. Planar measurements are best obtained with collimated light sheets, the maximum physical dimension of which is typically limited to around 50 mm for readily available optics. Ability to increase the sheet size is also limited by available laser power and by the reduction in spatial resolution associated with a larger measurement area and the size of a given pixel array on a CCD detector. Nevertheless, these challenges can be expected to diminish with advances in optical technology, as high-powered lasers become cheaper and as imaging detectors are developed with increasing spatial and dynamic resolution.

While the challenge of increasing the scale of the facility on measurement resolution is common to reacting and non-reacting facilities, the challenge of increased background interference is unique to combustion. The accuracy of a laser-based measurement depends on the strength of the signal relative to the background optical noise. The background interference, I_b, comprises components both from the flame and the furnace walls, and can be estimated to scale as follows:

$$I_b \approx \epsilon_F \sigma A_F \left(T_F^4 - T_{amb}^4\right) + \epsilon_W \sigma A_W \left(T_W^4 - T_{amb}^4\right) \tag{3}$$

Here ϵ_F and ϵ_W are the emissivities of the flame and furnace walls, respectively, σ is the Stefan-Boltzmann constant, A_F is the projected area of the flame, A_W the area of the furnace wall viewed by the imaging device,

while T_F and T_W are the temperatures of the flame and furnace walls.

Most measurements in a laboratory are performed in open flames, avoiding the interference from a wall entirely. This cannot be avoided in many realistic flames. The squared dependence of background interference with the size of the flame and path-length highlights the increased difficulty in providing reliable measurements at realistic scale. Finally, the background interference from the flame depends on both its temperature and emissivity. Most practical flames operate at elevated temperature relative to most laboratory flames, owing to the combustion air being preheated. Furthermore, the emissivity of a flame is dominated by the presence of particles, and in particular of soot. The volume fraction of soot within a flame, f_v, scales inversely with the intensity of strain in a flame [33]. While local strain rates fluctuate with both space and time, they can be characterised by the exit flame strain rate, u/d, or its inverse the characteristic flame time [34] or by the global mixing rate [35]. It is readily apparent that this corresponds to $1/\tau_{res}$. Returning to Table 2, it is evident that global strain rates decrease dramatically (typically by from one to two orders of magnitude, depending on the scaling approach) with increased scale. The reduced global strain rate significantly increases the presence of soot in flames of realistic scale, and so also the background interference.

The combination of the above challenges associated with increased scale means that complete detailed and simultaneous measurements have only been performed in small-scale laboratory flames with ambient temperature air, no soot and without the presence of furnace walls [36, 37]. Nevertheless, significant progress has been made in the development of measurement approaches

of key parameters within larger scale flames.

A range of optical measurements has been performed in furnaces. In some cases the optical access is provided through viewports in the walls of the furnace. However another approach is to insert optical components into the flame, using water-cooled jackets to protect them. This has been termed "semi-intrusive" devices. The International Flame Research Foundation plays a leading role in developing semi-intrusive systems first for single point LDV systems [38] and then for planar imaging [39]. More recently Sandia National Laboratory has developed a water-cooled probe to transfer an image to an ICCD camera via a fibre-optical coupling for measurements of soot volume fraction in a metre-scale pool fire [40].

Another ongoing challenge related to the investigation of practical reacting flows is the interaction of the reacting flows with the walls of a furnace or combustion chamber. Depending on the type of device, the vessel walls may be substantially hotter (*e.g.* a refractory quarl) or colder (*e.g.* boiler tubes and cylinder walls) than the adjacent reacting flow. The boundary layer therefore exhibits high gradients in both temperature and velocity. Hence these regions have a significant influence on heat loss or gain, local extinction and/or ignition, flame stability and pollutant formation. Most laser-based techniques are unable to resolve the boundary layer close to the wall, owing to the strong interference by scattering that occurs close to a surface. This issue is still unresolved and requires further attention.

4. Measurement of temperature

Temperature is a dominant parameter in combustion processes and the key parameter in radiation heat transfer owing to its fourth power influence on heat transfer. It characterises the enthalpy of reaction and controls many of the important chemical and physical processes, which also influence composition. A variety of laser-based thermometry techniques have been developed [2]. However, most of these are limited to clean combustion environments and are not applicable in the presence of particles, such as dust, coal, biomass and soot. Absorption, scatter and other interferences due to the presence of soot and its precursors prevent many laser diagnostic techniques from being applied reliably. This limits the capacity to investigate and understand many systems of practical significance.

A relatively simple, yet useful, laser-based thermometry technique is Rayleigh scattering. The elastic scatter of light from molecules gives a measure of the total number density, which when coupled with ideal gas law, allows the temperature to be deduced. Rayleigh scattering, however, is highly susceptible to interference from the elastically scattered light from particles (Mie scattering) and surfaces. It can therefore only be employed under very clean, particle-free environments, which limits its applicability in practical combustion systems [41]. Filtered Rayleigh scattering (FRS) is an extension of the conventional Rayleigh scattering that was first proposed by Miles *et al.* [42] and widely investigated subsequently [41, 43–46]. The FRS technique utilises a narrow band filter at the centre of the frequency of a single mode laser to reject interference that is spectrally identical to the incident light. The FRS technique has been primarily used with molecular-iodine

filters paired with frequency doubled single mode Nd:YAG lasers. The unfiltered component of the pressure- and/or temperature-broadened signal of the scattered light unfiltered is subsequently used for thermography. The broadening of the Rayleigh line-shape in relation to an iodine filter is apparent in Figure 2, reproduced from Hoffman *et al.* [41]. The filter allows temperature imaging to be performed in the presence of strong elastic scatter that would otherwise obscure the Rayleigh scattered signal, although its potential in highly particle-laden flows is questionable. An example of the impact of the filter on the Rayleigh scatter from a mildly sooty, slightly premixed methane-air flame may be seen in Figure 3, reproduced from Hofmann *et al.* [44]. It is apparent in the bottom image (collected without a filter) that the scattering from the soot sheets dominate the image. When the filter is used (top figure) the temperature may be determined from FRS with minimal interference from the soot. Despite the improved capability of FRS over unfiltered Rayleigh scattering, it remains susceptible to variation in the Rayleigh cross-section across the reaction zone, which can be difficult to account for in turbulent imaging applications.

One approach to circumvent problems associated with elastic scatter is to employ the inelastic Raman scattering for thermometry [47]. However, the inherently low signal from spontaneous Raman does restrict its application. It is typically limited to point or line measurements. Nonetheless, pointwise temperature measurements have been collected in practical devices in soot-free environments, such as a premixed gas turbine swirling flame [48].

Offering stronger signal due to its coherent nature, Coherent Anti-Stokes Raman Spectroscopy (CARS) is more applicable to thermometry in lumi-

nous and particle laden flows [49]. Indeed CARS has been the most widely used thermometry technique for harsh combustion environments, such as gas turbine combustors [50], liquid fuel combustors [51] and sooty turbulent pool fires [46].

The basic operating principle of CARS [2, 47] involves the use of three laser beams (typically two of the same wavelength) that interact in the measurement volume to generate the signal (as a fourth beam) as a result of the third-order nonlinear susceptibility [2, 47]. A 'pump' beam at frequency ω_{pu} (non-resonant to molecular transitions) excites a virtual level. By tuning a second Stokes beam to frequency ω_S, where ω_{pu}-ω_S corresponds to a vibrational or rotational transition of the molecule, Raman resonance occurs. A third, 'probe' beam (ω_{pr}) is then used to generate a coherent CARS signal at $\omega_{CARS} = \omega_{pu} - \omega_S + \omega_{pr}$. By scanning the Stokes beam across the Raman transitions of the molecule, the spectral shape is used to determine the temperature. Scanning of the Stokes wavelength may be performed on a shot-by-shot basis, or alternatively a broadband laser enables single-shot spectra to be generated. The advent of femto-second lasers is particularly important for the continued development of single-shot CARS for turbulent environments. The inherent frequency spread of femto-second laser pulses can be used to excite multiple pump-Stokes pairs, as shown in Figure 4 [52].

A key advantage of the CARS technique for assessing practical systems results from the frequency shift in the signal relative to the excitation beams. This allows filtering to separate out the influence of scattered interference from soot. Careful selection of the excitation scheme is necessary to minimise soot interferences [53]. Approaches include a dual-pump CARS technique

with an annular phase matching geometry (USED CARS) [54] and shifted vibrational CARS [55]. In exciting N_2, O_2 and CO_2, this approach has the further advantage of avoiding seeding, and accessing species that are widely present in the flame. In addition the signal is coherent, allowing the signal to noise be increased by moving the collection optics further from the flame (since the background is incoherent), so attenuates with r^2. The use of short-pulse (sub-nanosecond) laser excitation has the further advantage of allowing the signal to be delayed relative to the scattered interference, providing high signal quality and effectively eliminating interference from soot [56].

Despite these advantages, CARS suffers from a number of disadvantages for application in turbulent flames. The necessity for line-of-sight optical access and the experimental complexity are practical limitations. However, more fundamentally, the beam configuration results in an elongated probe volume of typical dimensions 1.5 mm×60 µm [51]. This lack of high spatial fidelity in comparison to planar techniques has previously been recognised as restricting the generic application of CARS [2]. In addition, its reliance on three beams with different optical paths means that the method is subject to differential beam steering and differential attenuation in a turbulent environment, especially in the presence of soot. Finally, the method has hitherto been limited to single point and no method to extend it to allow planar measurement has been proposed, as is desirable for investigation of turbulent systems and compatibility with other planar measurements.

The signal collected from laser-induced fluorescence (LIF) is typically shifted from that of the excitation, allowing it to be separated from the scattered interference that plagues Raman and Rayleigh scattering. The

fluorescence signal is typically quite strong, making LIF better suited to two-dimensional imaging than Raman and Rayleigh techniques [22]. Various strategies exist for thermometry, all of which are based upon the species' population according to the Boltzmann distribution. The species of excitation can be naturally occurring or artificially seeded.

The use of *in-situ* species (*e.g.* OH, CN, CH) for LIF thermometry is limited because of their low concentrations, and the narrow regions within the flame in which they typically exist. Of the naturally occurring species within a flame, the OH radical has been most commonly used [57–61]. In nonpremixed flames, OH only exists over a small range of temperature and mixture fraction, and so is not well suited for general measurements [62]. Furthermore, in fuel-rich flames the OH concentration is low, making it poorly suited to simultaneous measurements with soot, which is typically found in the fuel-rich size of the reaction zone [63]. Nitric oxide (NO), which is formed natively during the combustion process, could potentially be used for thermometry, though additional NO is typically added to the inlet streams to give a much improved signal quality [57, 64]. However, in the presence of soot, background interferences can lead to a significant error in two-line NO-LIF thermometry [65]. Multi-line approaches for NO thermometry alleviate issues with background [66], but at the cost of being restricted to averaged results. The excitation wavelengths required for NO (around 226 nm) can also cause problems with interference and attenuation, and pressure broadening of the excitation lines leads to spectral overlap [67]. Furthermore, in fuel-rich flames, NO is consumed due to reburn reactions, leading to a loss of signal [64, 68, 69]. As an alternative to naturally occurring species, a wide

range of seeded species can be introduced, of which organic molecules are most common [70].

The accuracy of single-wavelength LIF thermometry relies on the knowledge of the quenching species densities and quenching rate constant, since the spectra and intensity of LIF are influenced by the variation in collisional processes across reaction zone. However, this problem can be avoided by taking the ratio of two excitation/detection wavelengths [22, 71]. The number density, absorbing species concentration and the collisional quenching dependencies that are often associated with single line LIF technique are also nullified by taking the ratio of the fluorescence signals. Figure 5 presents an example of two-line LIF using 3-pentanone as a fuel tracer in a two-stroke internal combustion engine [72]. It is also possible to employ single laser excitation and detection at two different wavelengths, *e.g.* with toluene as the tracer [73]. However, as with many fuel tracers, 3-pentanone and toluene are consumed in the reaction zone, and so measurements are only possible in the unburned region.

Alternative two-line fluorescent techniques have also been explored. For aqueous systems, the use of two different laser dyes has been proposed [74]. For simultaneous thermometry and velocimetry, the use of liquid-crystals has also been proposed [75]. However, their relevance to turbulent flames is not clear, since they have a limited temporal response and do not survive the combustion environment. Two-line phosphorescence using ZnO:Zn & ZnO:Ga has also been reported, with claims of short lifetimes enabling elimination of background interference [76]. Temperature measurements using naphthalene has also recently been reported [77]. However, the feasibility

of these techniques in practical flame environments is yet to be adequately demonstrated.

Of the laser-based thermometry techniques, two-line atomic fluorescence (TLAF) is potentially one of the most suitable for sooting environments, especially for two-dimensional imaging [78]. TLAF follows the same principle as other LIF-based thermometry techniques, but employs a seeded atomic species. Some advantages of the TLAF technique include good sensitivity over a temperature range relevant to combustion, insensitivity to collisional quenching effects and capacity to separate the inelastic fluorescence from interference by spurious scattering [79–82].

Of the atomic species available, indium seeded into the flame has been identified as a suitable thermometry species for TLAF [83]. Indium has good sensitivity over the temperature range 800 to 2800 K [84] and both of the wavelengths are in the visible spectrum (*viz.* 410 nm and 450 nm), where interferences are less pronounced than in the UV range typically employed for excitation. Feasibility studies [62, 80] have shown that TLAF with indium holds promise for temperature measurement in a highly sooting environment. The indium is typically introduced to the system as indium chloride dissolved in water. Within the flame front, neutral indium atoms are generated, which are spectroscopically probed using the TLAF technique.

The strong transitions of atoms are easily saturated. To remain in the linear excitation regime, which is required for insensitivity to collisional quenching effects, the laser energy must be limited to low fluences. This leads to weak signal strength, and so affected by low signal-to-noise ratio, thus time-averaging is typically necessary. To circumvent this issue, the possibility of

extending the technique to higher laser energies, so called nonlinear excitation regime TLAF (NTLAF) has been undertaken to extend the work to single-shot imaging, initially under premixed conditions without the presence of soot [78, 85]. Still more recently single-shot imaging of temperature has been demonstrated in the presence of soot, and performed simultaneously with LII of soot volume fraction, as shown in Figure 6 [86].

The strong signal strength of the NTLAF results in good signal to noise ratios and measurement uncertainty of about 60 K within its operating range. However, the highly reactive nature of the indium ions means that they are readily consumed under oxidising environments. This limits the range of mixture fraction for which measurements can be performed to $\Phi>0.9$. Note that the consumption of indium does not directly influence the accuracy of the temperature measurements, which is determined from the ratio of the intensity of the two colours (Stokes and Anti-Stokes). However it may increase the measurement uncertainty by reducing the signal relative to noise. This is a fundamental limitation of the method. However, further advances in seeding approaches are potentially achievable, which may allow the method to be extended further into the lean regime beyond its present limitation of $\Phi>0.9$ and to temperatures below its present limit of 800 K [78, 86, 87]. Measurements to date have only been demonstrated under conditions of relatively low soot volume fraction, owing to interference due to condensed species and/or PAH on the fuel-rich side of the soot particles [88]. Recent analysis of this interference suggests that the correction for these interferences is realistic. Hence, while measurements under high loading are yet to be demonstrated, this can be anticipated in the near future.

5. Measurement of mixture fraction

Mixing plays a key role in radiation heat transfer through its influence on composition, and so on emissivity, which depends significantly on the presence of specular gases such as CO_2 and H_2O, and of soot [1]. Mixing also influences the control and emission of pollutants. Both large scale and molecular mixing are important in determining flame shape, stability and burning characteristics. This role is less important in premixed flames, although turbulence can still play a role through strain and residence time.

Mixture fraction, ξ, is a conserved scalar which represent the mass fraction of reactant(s) that originated in the fuel stream. This scalar is used in many combustion models to reduce the number of variables needed to represent the mixing process and, through it, the local flame structure. Models such as Conditional Moment Closure, CMC, and the Laminar Flamelets Model are based on the mixture fraction, which is calculated from species concentration [89–91].

The process of model development and validation requires reliable experimental measurements of mixture fraction in reacting flows that have been performed under conditions where experimental and computational data can be directly compared. Such data allows researchers to focus on the compositional structure without the complication of flame shape and size. These measurements are usually conducted on one or more of the key fuel components that are spectroscopically accessible and whose kinetics are well understood. Measurements are done either through intrusive sampling probes and gas chromatography or through temporally and spatially resolved laser based techniques. In the latter, some challenges are faced in accurately measuring

the mixture fraction in all parts of the flame.

It is possible to measure the key species and deduce the mixture fraction based on elemental conservation. However, such measurements are restricted to point measurements and 1-D line measurements of late. Planar imaging of the fuel has two main challenges, which are the early dissociation of the fuel (such as CH_4), on the rich side of stoichiometric, and the effect of differential diffusion. In addition imaging of the fuel alone restricts the measurements to the rich side of the flame. Fuel dissociation results in very low concentration of the probed species and results in poor quality signal around stoichiometric conditions. Differential diffusion arises when molecular diffusion is more significant in one component of the mixture than the others, and is especially for multi-component fuels containing H_2. This leads to a misrepresentation of the mixing when only one part of the fuel composition is measured.

An alternative to the direct measurement of all of the fuel species is the use of a fuel tracer. The most widely employed tracer species employed to date for this purpose are fuels such as acetone, 3-pentanone or toluene, although more recently Krypton has emerged as an exciting alternative, at least for gaseous fuels [92].

The fuel-based tracers are most suitable for liquid fuels, but also suffer from a range of systematic errors that limit their applicability to the measurement of fuel mass fraction. These limitations include the difference between spray formation and evaporation of the fuel and the tracer (noting that these tracers are typically liquid), different ignition chemistry and their breakdown at temperatures well below that of the reaction zone. Also, their quantification depends on understanding the effect of molecular quenching, correction

for interferences and the need to quantify the temperature to determine the population distribution of electrons, known as the Boltzmann distribution. Higher pressures add further complexity to resolve.

Schulz and Sick [70] reviewed the techniques used to measure fuel mass fraction and temperature by LIF, with a focus on application in internal combustion engines and at high pressure. They concluded that LIF is one of the more robust techniques for measuring fuel concentration in such environments, and also in the presence of particles. They noted that the selectivity of the LIF technique allows the probing of the specific species, either added as tracers or found naturally in the flame. Shultz and Sick have also highlighted the difficulties associated with the quantification of the measured species and their relevance to the actual fuel mass fraction. They further identified the lack of discrimination between liquid and gas phase signals, as a remaining challenge for tracer-LIF in many applications. Indeed the measurement of mixture fraction in liquid and solid fuels in reacting system remains a challenge for all techniques. The phase transition hampers the accurate measurement of the fuel in the gas phase and the presence of droplets and particles interferes with most laser diagnostics techniques [93]. Finally the presence of soot in the flame adds both further complexity due to laser beam scatter and attenuation due to the dense medium of soot particle and fluorescence and chemiluminescence from the hot soot particles, as noted above.

Despite the above limitations and complexities, many valuable measurements of mixture fraction and temperature in "clean" gaseous turbulent non-premixed flames have been reported in the last two decades [36, 94]. Such

measurements involve an elaborate experimental arrangement and extensive experimental procedures for calibration and to correct for the various interferences. Figures 7 and 8 are examples of such arrangements for two dimensional and 1-D line configurations, respectively. These data have contributed significantly to the understanding of the turbulent mixing characteristics (through mixture fraction) and their dependence on controlling parameters such as Reynolds number, stoichiometric mixture fraction and the type of fuel. Figure 9 shows detailed planar structure of the mixing field, OH and temperature, using the Raman, LIF and Rayleigh techniques respectively [37]. These data were taken at different heights in a bluff body stabilised turbulent nonpremixed CH_4/H_2 flames and show the impact of the vortical structure shed from the edge of the bluff body on the structure of the flame downstream.

The capacity to measure mass fractions of major species, temperature and minor species have formed the basis of an international workshop on turbulent nonpremixed flame, the TNF workshop, which capitalises on the wealth of data available for model validation and development [13]. Invariably, these major species data have been collected using the Raman scattering technique.

The Raman scattering technique is used to measure species concentration in gaseous flows. This technique can probe a specific species but suffers from weak signal and cannot be used in any environment where particles or droplets are present. The Raman signal can also suffer from other interferences such as those from high hydrocarbons and overlap between the Raman lines. Single-point [36] 1-D line [95] and 2-D planar imaging [37] measurements have been reported in the past. These data provided valuable insight into the fate of the fuel in a variety of turbulent jet flames and fuels and its

impact on the reaction zone structure.

Of late, two comparatively similar systems have been developed at Sandia National Laboratories [95] and Darmstadt University [96] to overcome the limitations of the Raman technique. These systems contain four combined Nd:YAG lasers to maximize the fluence in the probe volume and stretch the pulse over 40 ns. Another innovative feature is a spinning wheel system with a small slit to gate the signal and minimise interference from the flame, while synchronising the exposure with the laser pulse. This approach has helped improve the signal to noise substantially and reduce the noise associated with an electronic intensifier. An increasingly utilised extension involves the modelling of the Raman spectra [97] to provide the temperature-dependent calibration and a correction for the cross talk between the different Raman responses for the different species. These new systems have underpinned capacity to provide resolved measurements of scalar dissipation [17] and offer potential to extend the Raman capabilities to flames with small amounts of soot or to larger flames.

The measurement of mixture fraction will remain a key requirement for future research to characterise non-premixed flames. The existing laser diagnostics techniques are still limited in its scope to deal with many of the issues associated with practical flames, notably those that contain soot and particulates.

The method with the greatest promise for conserved scalar measurement in strongly radiating flows is the recently proposed measurement of Kyrpton by two-photon fluorescence. As a noble gas, Krypton is well suited to conserved scalar measurements, being very stable in a flame, although it has

the disadvantage of being expensive. It is also optically accessible, albeit with some challenges. The two photon technique means that the collection wavelength at 760 nm is very different from the excitation wavelength of 215 nm, making it well suited to separation of the signal from laser induced interference by filtering. The signal is subject to quenching, so an iterative approach combined with the measurement of temperature is required to determine mixture fraction. The method has recently been validated against the established Raman-Rayleigh methods in a non-premixed flame [92], but has yet to be assessed in flames with soot. It is also well suited to planar imaging.

6. Measurement of soot

The broad-band incandescent radiation from soot, where it is present, dominates over the narrow-band energy from gaseous species, making its measurement of paramount importance. Laser-induced incandescence is currently the most versatile technique for quantitative measurement of soot volume fraction, f_v. The technique is based on the property of soot particles that causes them to absorb laser radiation at any wavelength. Laser energy is introduced at sufficient fluxes to heat the soot particles to temperatures far above the flame temperature. Hence these laser heated soot particles will emit radiation at shorter wavelengths than the flame, allowing its separation from the background [2, 98]. The attraction of this technique is that the detected LII signal, S_{LII}, is linearly proportional to the f_v. This enables spatial and temporal quantitative soot measurements with the use of a high-energy pulsed laser coupled with suitable photo detection equipment as

shown in Figure 10. The detected S_{LII} counts need to be calibrated, which may be achieved using either *in-situ*, or *ex-situ* methods such as laser extinction (LE) [99, 100] or by gravimetric sampling [101]. The LE technique, preformed in a well-controlled laminar premixed flames (as shown in Figure 11) using continuous-wave lasers, is used widely to obtain the calibration factor. The value of the measured laser extinction, K_{ext}, is directly related to the soot volume fraction, which can be described by the following equation:

$$K_{ext} = -\frac{\pi^2}{\lambda}\mathrm{Im}\left(\frac{m^2-1}{m^2+2}\right)Nd^3 \ . \tag{4}$$

N, d, λ and m are defined here as the number density, particle diameter, laser wavelength and a complex number which represents the refractive index, respectively. Equation 4 is valid in the Rayleigh regime where the soot diameters are expected to be in the range of $d_p<0.3\lambda/\pi$. This limits the range of soot diameters to >50 nm, >60 nm and >101 nm, for laser wavelengths of 532 nm, 632 nm and 1064 nm, respectively. The presence of polycyclic aromatic hydrocarbons (PAHs) influences the line of sight LE and may cause an overestimation on the soot volume fraction profiles by an order of magnitude. Bengtsson and Alden [102] concluded that, at low burner heights in a laminar flame, the presence of PAHs emits strong fluorescence signals that increase with C/O ratio. Zerbs *et al.* [103] report on the influence of wavelength on the measured extinction for calibration of LII. They recommend calibration at long wavelengths (*e.g.* 1064 nm) for the laser extinction measurements to reduce the laser absorption by molecular species (*e.g.* PAH) in the flame.

Recently LII has been used to obtain f_v in three different flames to investigate the effect of global mixing [35]. Very recently, Qamar *et al.* [104] re-

ported experimental measurements of f_v in piloted turbulent diffusion flames. Henriksen *et al.* [105] have also reported LII measurements in a highly sooty pool fire. They also reported simultaneous images of f_v and OH. Lee *et al.* [106] reported simultaneous measurements of f_v and OH in a turbulent flame of ethylene.

The application of LII in turbulent flames, in presence of soot, requires careful consideration. This is because these flames are generally large and contains high temperature gradients. The soot distribution in the flame and the temperature gradients will influence the laser beam propagating throughout the flame, causing both beam steering and diffraction effects. This leads to an unavoidable degradation in spatial resolution, typically in the range of 500% for a flame width of order 0.2 m [107]. Zerbs *et al.* [103] note that beam steering, due to the combined effects of turbulence, thermal gradients, pre-heat and pressure, implies that a spatial resolution below 1 mm in the dimension of the laser sheet thickness is not realistic under technical conditions. In addition to the spatial resolution degrading, the magnitude of computed f_v values will also be affected by these issues. Another complexity of turbulent flames is that soot is present at different diameters and morphologies, associated with different ages that can cause diameters to exceed the restricted soot diameter values addressed in Equation 4. To minimise this effect, a longer wavelength for the laser extinction measurements is desirable, which also reduces the laser absorption by molecular species [103].

7. Measurements of droplets

Turbulent flows transporting reacting droplets are not only of great practical significance in their own right, they represent an intermediate step in complexity between gaseous and particulate fuels. This is as true for the radiative heat transfer processes as the other process of combustion. Droplets have a number of properties that can be exploited in their measurement within reacting environments. Firstly, being spherical allows the exploitation of a range of methodologies that require sphericity, such as phase Doppler particle anemometry, PDPA, and particle sizing from scattering [108]. PDPA is a single point technique that will also provide, for each droplet, all three components of velocity, as well as diameter. A wide range of single-point measurements have been employed of turbulent reacting flows with particles, including the series of well-characterised flames by Masri and co-workers [93].

However, multiple droplets within the measurement volume result in spurious results, or measurement inaccuracy. This sets the critical mass loading, above which the number of bad measurements exceeds a useful threshold and also results in a significant bias. By counting, the size distribution and mass loading of the droplets can be obtained. Laser sheet drop-sizing, LSD, measures simultaneously the scattered signal from one laser, which depends on d_p^2, and another on the fluorescence from another laser, which depends on d_p^3. Hence the ratio of these two signals can be used to measure diameter. While LSD has been used to provide measurement of mean diameter, Kalt *et al.* [109] have found that LSD is not useful in providing detailed statistics. This is because the cubic dependence of the fluorescence signal on droplet diameter means that it is not possible to obtain good resolution

of both large and small droplets simultaneously. That is, avoiding saturation from the large droplets results in too low a signal-to-noise ratio from the small droplets for reliable measurement. This method is also limited to isothermal environments, since the fluorescent species will also persist in the vapour phase, rendering the ratio irrelevant.

A range of liquid fuels are also suitable for fluorescence measurements. This has made acetone the fuel of choice for some investigations [93]. Alternatively, fluorescent materials such as toluene can be dissolved into other fuels for measurement of temperature and/or mixture fraction, as described above [70]. At the same time, such measurements cannot distinguish between the fluorescent species in the liquid and vapour phases [70]. Hence planar measurements of droplet size and number density are still not realistic under reacting conditions.

8. Measurements of particles

Most solid fuels, both of fossil or biomass origin, are burned in pulverised form, since the combustion intensity can be increased as particle size is reduced. The distribution and number density of coal particles as they disperse into a combustion chamber influences the location of the ignition plane, the distributions of temperature and mixture fraction and hence also the radiation heat transfer and pollutant emissions [110]. The large numbers of particles, combined with the presence of soot they produce, make radiation from these flames even more dominant than in gas flames. Knowledge of these parameters is thus central to the optimisation of all aspects of such systems.

In pulverised fuel (PF) combustion systems, the fuel is typically crushed to produce particles with a log-normal size distribution that spans two to three orders of magnitude. The mean size is typically around 60 µm, the largest particles are typically around 300 µm and the smallest particles numbers are <1 µm. This size allows them to be conveyed pneumatically and also provides a high surface area to volume ratio for rapid combustion. Such particles are typically conveyed in the "dilute" phase, *i.e.* at velocities sufficient to prevent particles from settling to the floor of the duct, with mass loadings of less than 10 $kg_{particles}/kg_{air}$ but more commonly at around 1 $kg_{particles}/kg_{air}$ [111]. Under these conditions the volume fraction of particles is typically about 1% and 0.1% respectively. However, the particles disperse as they move from the conveying system into, and through, the flame, resulting in significantly lower number densities in much of the flame. Importantly, the cubic relationship between particle numbers and mass causes the fine particles to dominate particle numbers. For example, a typical coal of density 1300 kg/m^3 and a mass loading ratio of 10 would have 10^13 particles per m^3, based on 10 µm diameter.

It is difficult to measure particle numbers accurately with such a wide size distribution. This is because intensity of the scattered signal from a laser scales approximately with d_p^2 when the particle is much larger that the wavelength of light. This scaling causes scattered signal to be dominated by the large particles. The effects of optical attenuation are also very significant in investigations of conditions of relevance to pulverised fuel flames. These effects have typically limited previous laser-scattering images from pulverised coal particles to providing qualitative insight, as in the 2 MW,

pilot-scale combustion investigations of Smith *et al.* [112]. The combined effects of attenuation and signal trapping have also limited most previous investigations of instantaneous particle number densities to either single point methods [113] or to planar investigations under dilute conditions where the effects of attenuation can be neglected [114]. Nevertheless, the attenuation in PF environments is typically not so great as to prevent reasonable signal from throughout the flame [112]. Hence it is realistic to consider that reliable measurements are possible under conditions of relevance to practical pulverised fuel combustion.

One important step in the development of reliable planar measurements of particle distributions is the shot-by-shot correction for in-plane attenuation. Kalt *et al.* [115, 116] have developed a ray-tracing approach. They applied an iterative correction to the Beer-Lambert Law of gaseous absorption, *i.e.* by ignoring effects of diffraction. Specifically, they derived the following correction:

$$\varphi_P = C_K(\overline{\pi r_P^2}) n_P I' \ . \tag{5}$$

Here φ_P is the detected signal from the particles, C_K is a constant of correction that can be applied for the entire optical arrangement, $\overline{\pi r_P^2}$ is the average particle cross-sectional area available to scatter signal, n_P is the number of particles and I' is the laser intensity entering the measurement volume. This can be applied in differential form using ray tracing from pixel to pixel, as is illustrated in Figure 12. It can also be applied in modified form to divergent light sheets.

Diverging laser sheets cause some additional complications. Firstly, the

sheet divergence causes both a drop in the local laser fluence [J/mm^2] and an increase in the dynamic range of fluence in the image plane. Secondly, the particles cast conical shadows rather than cylindrical shadows. The influence of particles on the extinction of the diverging sheet depends on the particle position with respect to the virtual origin of the laser sheet (Figure 13). The extrusion of square image volumes allows ray tracing through the laser sheet. The simplified 1-D model of collimated attenuation corrections that account for divergence for a 1-D ray, constructed by interpolation for each pixel back to the laser source (virtual origin), is shown schematically in Figure 14.

Importantly, Kalt *et al.* also assessed the effect of signal trapping, *i.e.* the attenuation of signal between the measurement volume and the detection optics. They found that, using sufficiently large optics, the effects of signal trapping can be corrected based only on the mean values to provide a total accuracy of typically 3%, or up to 10% for the case where the transmittance is only 50%, *i.e.* where half of the energy has been attenuated. However, to date, no method to account for non spherical particles has been developed.

Furthermore, many biomass particles tend to be fibrous in shape, which makes their aerodynamic behaviour even more complex. The drag depends on orientation, aspect ratio and rotational velocity. Their motions are now becoming to be better understood under settling [117, 118], but are only beginning to be investigated in detail in non-reacting turbulent environments [119]. The measurement of fibres is also significantly more difficult than of spheres, since the intensity of the scattered signal also depends on the orientation of the fibre within the light sheet. These challenges have limited the conditions in which the most detailed data-sets are available to relatively

simple systems. Hence the challenge to provide detailed measurements under conditions of direct relevance to turbulent combustion remains significant.

Another exciting recent development for the planar measurement of densely laden flows of particles is Structured Laser Illumination Planar Imaging (SLIPI) [120, 121]. This method allows removal of the influence of secondary scattering as the laser propagates through a particle laden flow. It employs three laser sheets, each slightly separated in time and each with a sinusoidal spatial variation in the distribution in intensity, slightly offset from each other. The sinusoidal variation in spatial intensity, generated by the use of a grating, is illustrated in Figure 15. Each image comprises the superposition of the primary signal, generated only by the direct scattering of the laser sheet, with the secondary scattering, generated by multiple scattering events. The primary signal is identical in each sheet, except for the variation in intensity, while the secondary scattering is random. The appropriate recombination of the three images allows the random scattering to be removed, as illustrated in Figure 16.

9. Measurement of velocity

It is well established that strain rate is a major controlling parameter for the formation of soot, while also influencing temperature and mixture fraction. However, laser based velocity measurements in turbulent flames with soot suffer from large interferences, which has hindered any attempt of such measurements in the past. Novel investigations are therefore required to ensure that the soot (which is not a flow tracer, being both produced and consumed) does not bias measurements by Particle Image Velocimetry,

PIV, or LDA. Likewise, the simultaneous measurements of velocity and soot volume fraction have been hindered by the need to demonstrate that the PIV seed particles do not interfere with the LII measurement.

To confirm that reliable optical discrimination between the two measurements is possible, the authors have performed a preliminary investigation in a laminar ethylene diffusion-flame issuing from a 10 mm nozzle at 1 m/s (Figure 17). Both the fuel and air were seeded with 0.5 µm aluminium oxide particles as flow tracers for the PIV and illuminated at 532 nm from a Quantel Twins B PIV double pulsed Nd:YAG laser, operated at 300 mJ/pulse. A 430 nm interference filter was found to be sufficient to suppress any interference from the seed particles on the LII image to below detectable limits. This is demonstrated in Figure 17b, since LII signal is found only in the thin sheet of the flame, where the soot is known to be found. This verifies that the use of PIV will not interfere with the LII measurement here, and any interference will be even less with 1064 nm.

A polarising filter was sufficient to suppress the scattering from the soot to background levels, to avoid interference of soot on the PIV measurement. The Mie-scattering efficiency of the Aluminium Oxide particles used in these preliminary investigations is reduced by a factor of approximately 8 at the temperatures in the flame-front relative to ambient. This results in a low signal intensity of the Mie-scattering in the flame zone, as shown in Figure 17c. The replacement of aluminium oxide with particles of higher scattering efficiency at elevated temperature, such as magnesium oxide, can further enhance measurements. Despite the draw backs of Aluminium Oxide, Figure 17d demonstrates that it provides sufficient Mie-scattering signal to

conduct PIV under laminar conditions. Discrimination can also be enhanced by the use of a better camera.

10. Components of radiation propagation

The corrections for the attenuation of light described in § 8 can be extended to provide direct planar measurement of all components of radiation through a scattering-absorbing medium on a shot-to-shot basis. Such measurements have not been reported previously and have potential to provide an important step in model development and validation. The attenuation corrections can be used to quantify particle concentration if the appropriate scaling constant, C_K, can be found. This scaling constant, which represents the detector sensitivity to scattered radiation can be determined for a given optical arrangement — either in advance by testing against a known concentration of particles, or by measuring the intensity of the transmitted laser sheet and iteratively determining a C_K value that yields the same overall transmission. The quantitative processing of Mie-scattering nephelometry data will then provide laser sheet fluence, particle concentration and corrections for local laser intensity due to absorption of the laser sheet and divergence of the beam. Figure 18 [122] shows how these components can be used to determine the components of radiation collectively scattered and absorbed by the particulate medium. The diffusely scattered component, which depends on the surface properties and diameter, is typically dominant (around 96%) while the absorbed component very much weaker. For sufficiently large particles the scattered light is no longer coherent, becomes depolarised, and contributes to the multiple scattering signal and background radiation lev-

els. The influence of the absorbed radiation depends on its composition and environment and can result in an increase its temperature and/or a change in phase or composition. However, the wavelength of the emitted radiation from a particle is typically broad-band and temperature dependant, and can be separated from the narrow-band scattered radiation by use of a sufficiently high wavelength laser.

It is a relatively easy proposition to measure the laser power shot-to-shot, as the data is collected. If the total power and laser sheet energy profile are known then the scattered and absorbed radiative components can be quantified on a shot-to-shot basis, as illustrated in Figure 18.

11. Conclusions

A number of complementary planar laser diagnostic techniques have recently emerged that together offer the potential for a breakthrough in capability to investigate strongly radiating turbulent reacting flows. Notably, nonlinear two line atomic fluorescence (NTLAF) has been demonstrated for the measurement of gas-phase temperature in flames with soot, while two photon fluorescence of krypton is emerging for the measurement of mixture fraction. Such measurements have not previously been possible under conditions of strong interference, notably from the presence of soot and its precursors. Similarly, two planar measurement techniques have recently emerged to enable measurement of particle volume fraction under much higher loadings than previously possible. One employs ray tracing to account for single-shot attenuation of the primary laser sheet, while the other employs structured illumination to remove much of the secondary scattering. Furthermore, these

methods could, in principle, be applied simultaneously, although this is yet to be done. Hence, they offer the potential to enable detailed measurement of the coupled processes of turbulence, combustion and radiation. Such coupling is particularly significant in strongly radiating flows, notably involving soot, making these flows too complex to model without the use of a range of simplifying assumption.

For *in-situ* laser-based thermometry, perhaps the best established method is Rayleigh scattering, whose simplicity continues to make it the method of choice for clean environments. However its vulnerability to interference from scattering makes it poorly suited to investigate strongly radiating flows, such as those involving soot. Of the established techniques, the Coherent Anti-Stokes Raman Spectroscopy, CARS, offers the greatest capability in such environments. The use of pico-second lasers has recently been shown to enable good separation between signal and noise in the presence of soot. Nevertheless, CARS retains the disadvantages of a relatively large probe volume (*i.e.* moderate spatial resolution), which is linked to its vulnerability to differential beam steering, and to being poorly suited to planar measurement. The thermometry technique with greatest promise for planar and well-resolved measurement of temperature in the presence of soot and other fine particles is NTLAF. This method has recently been demonstrated to provide simultaneous measurement of temperature and soot volume fraction. While, to date, it has only been demonstrated under conditions of moderate soot loading. It is anticipated that corrections for interference will allow the range to be extended to high soot loadings also. Similarly the presently accessible temperature range is limited to 800 K$<T<$2800 K, and that of mixture

fraction to the range $0.9<\Phi<1.4$. These ranges are of primary immediate interest because they span the high temperature reaction zone, and with further development, it is anticipated that will be extended to a wider operating range.

For the measurement of mixture fraction in turbulent flames, Raman-Rayleigh techniques have proved to be well suited for clean flames. However, these methods are highly vulnerable to interference from the presence of soot (or other particles) and its precursors. Such measurements have presently also been limited to laboratory scale flames, although incremental refinement offers potential to extend them to larger physical scale. Tracer LIF is presently the only realistic technique by which to measure mixture fraction in the presence of particles, and is also well suited to planar measurements. Until recently, the tracers identified for measurement are themselves combustible, limiting their application to the relatively low temperature region on the fuel rich side of the reaction zone. The use of krypton as a tracer gas offers potential to overcome these disadvantages. Being inert, this tracer survives the reaction zone. It is also accessible with a two photon technique, which allows the signal to be separated from spurious scattering. Its recent emergence means that this method is yet to be demonstrated for turbulent flames with soot. Nevertheless, it has potential to allow the planar measurement of mixture fraction in strongly radiating turbulent flames.

Laser-induced incandescence has advanced to the stage where it has become the method of choice for the measurement of the volume fraction of soot and other nano-sized particles. It is well suited to planar measurements and has also been performed at large physical scale using water-cooled col-

lection optics coupled to the ICCD with a fibre-optical probe. Nevertheless, the technique is still under development owing to the complex nature of soot and the environment under which it is produced and consumed. For example, calibration remains a challenge in turbulent flames especially in those environments where some of the soot grows to sizes that take it outside of the Rayleigh limit. These issues can be minimised by the use of longer wavelength radiation. The use of 1064 nm, corresponding to the fundamental of a Nd:YAG laser, is therefore well suited both to minimising such losses and also avoiding interference from PAH and other soot precursors. Also, even in moderate scale turbulent flames, say of 200 mm diameter, the presence of soot, combined with other beam steering issues in turbulent flames, causes broadening of the laser sheet, and hence a loss in spatial resolution of some 500%.

A series of recent measurements have confirmed that LII can be performed simultaneously both with temperature (by NTLAF) and with the seed particles required for velocity measurements in the presence of soot, at least under laminar conditions. This provides confidence that simultaneous measurement of soot volume fraction, temperature and velocity is possible, although they are yet to be demonstrated all together in turbulent environment.

Measurement in the presence of soot or other particles also imposes the additional challenges of optical diffraction, attenuation and signal trapping. A number of approaches are being devised to incrementally advance capability to correct for these effects. However, such corrections retain some constraints and are presently limited to spherical particles. Also, the simultaneous planar measurement of particle size and particle number density is

presently not realistic under reacting conditions, even for liquid fuels. Hence substantial development is required before it is possible to provide detailed measurement of reacting flows under a wide range of conditions of practical relevance.

The simultaneous measurement of the scattered, absorbed and transmitted components of radiation has recently been demonstrated for spherical, non-reacting turbulent flows. This represents an important advance in capacity to develop detailed understanding of radiation propagation in more realistic conditions. This method could, in principle, be extended to reacting flows, but further work is required to account for non-spherical particle sizes and for non-uniform particle size distribution. It could also be combined with the SLIPI method, which allows removal of secondary scattering effects. Not only do these methods offer the advantage of spatially correlated information that is desirable for all turbulent systems, they also enable instantaneous ray-tracing, which is particularly valuable for radiation modelling. Such data, while not presently available in strongly radiating and turbulent environments owing to the challenges which particles impose on the measurements of key parameters such as temperature and mixture fraction, are now becoming possible.

These recent advances in measurement capability suggest that it will be possible to achieve significant advances in understanding and modelling capability of strongly radiating turbulent reacting flows through coordinated efforts, building on the great progress that has already made both in soot-free turbulent flames. Nevertheless, significant challenges remain to be overcome before such measurement are possible under many of the other conditions of

practical significance, including non-spherical particles, polydisperse particle size distributions and/or larger physical scale.

12. Acknowledgements

This research has been supported by the Australian Research Council and by the Centre for Energy Technology. Comments on an earlier version of the document by Dr A. Klimenko are also gratefully acknowledged.

References

[1] Coelho PJ. Numerical simulation of the interaction between turbulence and radiation in reactive flows. Prog Energy Combust Sci 2007; 33: 311-383.

[2] Kohse-Höinghaus K, Jeffries JB. Applied Combustion Diagnostics London, UK: Taylor & Francis; 2002.

[3] Viscanta R, Mengüc MP. Radiation heat transfer in combustion systems. Prog Energy Combust Sci 1987; 13: 37-160.

[4] Sims R, Schock R, Adegbululgbe A, Fenhann J, Konstantinaviciute I, Moomaw W, Nimir H, Schlamadinger B, Torres-Martínez J, Turner C, Uchiyama Y, Vuori S, Wamukonya N, Zhang X. In: Metz B, Davidson OR, Bosch PR, Dave R, Meyer LA. editors. Energy supply in climate change 2007: mitigation contribution of working group III fourth assessment report of the IPCC. Cambridge, UK; Cambridge University Press: 2007

[5] Z'Graggen A, Haueter P, Trommer D, Romero M, de Jesus JC, Steinfeld A. Hydrogen production by steam-gasification of petroleum coke using concentrated solar power - II Reactor design, testing, and modeling. Int J Hydrogen Energy 2006; 31: 797-811.

[6] Z'Graggen A, Steinfeld A. Hydrogen production by steam-gasification of carbonaceous materials using concentrated solar energy - V. Reactor modeling, optimization, and scale-up. Int J Hydrogen Energy 2008; 33: 5484-5492.

[7] Hawkes ER, Sankaran R, Sutherland JC, Chen JH. Scalar mixing in direct numerical simulations of temporally evolving plane jet flames with skeletal CO/H_2 kinetics. Proc Combust Inst 2007; 31: 1633-1640.

[8] Lignell DO, Chen JH, Smith PJ. Three-dimensional direct numerical simulation of soot formation and transport in a temporally-evolving, nonpremixed ethylene jet flame. Combust Flame 2008; 155: 316-333.

[9] Lu T, Law CK. Toward accommodating realistic fuel chemistry in large-scale computations. Prog Energy Combust Sci 2009; 35: 192-215.

[10] Battin-Leclerc F. Detailed chemical kinetic models for the low-temperature combustion of hydrocarbons with application to gasoline and diesel fuel surrogates. Prog Energy Combust Sci 2008; 34: 440-498.

[11] Barlow RS. Laser diagnostics and their interplay with computations to understand turbulent combustion. Proc Combust Inst 2007; 31: 49-75.

[12] Nathan GJ, Mi J, Alwahabi ZT, Newbold JR, Nobes DS. Impacts of

a jet's exit flow pattern on mixing and combustion performance. Prog Energy Combust Sci 2006; 32: 496-538.

[13] Turbulent Nonpremixed Flames Workshop. Available at http://public.ca.sandia.gov/TNF/abstract.html; 2010

[14] Mi J, Nathan GJ. The Influence of probe resolution on the measurement of a passive scalar and its derivatives. Exp Fluids 2003; 34: 687-696.

[15] Bilger RW. Some aspects of scalar dissipation. Flow Turb Comb 2004; 72: 93-114.

[16] Pitts WM, Richards CD, Levenson MS. Large and small-scale structures and their interactions in an axisymmetric jet. Report No. NISTIR 6393, National Institute of Standards and Technology, United States Department of Commerce Technology Administration:1999.

[17] Wang GH, Barlow RS, Clemens NT. Quantification of resolution and noise effects on thermal dissipation measurements in turbulent non-premixed jet flames. Proc Combust Inst 2007; 31: 1525-1532.

[18] Zimberg MJ, Frankel SH, Gore JP, Sivathanu YR. A study of coupled turbulent mixing, soot chemistry, and radiation effects using the linear eddy model. Combust Flame 1998; 113: 454-469.

[19] Xin Y, Gore JP, McGrattan KB, Rehm RG, Baum HR. Fire dynamics simulation of a turbulent buoyant flame using a mixure-fraction-based combustion model. Combust Flame 2005; 141: 329-335.

[20] Leung KM, Lindstedt RP, Jones WP. A simplified reaction mechanism for soot formation in non-premixed flame. Combust Flame 1991; 87: 289-305.

[21] Magnussen BF, Hjertager BH. On mathematical modeling of turbulent combustion with special emphasis on soot formation and combustion. Proc Combust Inst 1977; 16: 719-729.

[22] Lee MP, McMillin BK, Hanson RK. Temperature measurements in gases by use of planar laser-induced fluorescence imaging of NO. Appl Opt 1993; 32: 5379-5396.

[23] Kuhr C, Staus S, Schönbucher A. Modelling of the thermal radiation of pool fires. Prog Comp Fluid Dyn 2003; 3: 151-156.

[24] Spalding DB. Colloquium on modelling principals: The art of partial modelling. Proc Combust Inst 1963 ;9: 833-843.

[25] Weber R. Scaling characteristics of aerodynamics, heat transfer, and pollutant emissions in industrial flames. Proc Combust Inst 1996; 26: 3343-3354.

[26] Sayre A, Lallemant N, Dugué J, Weber R. Effect of radiation on Nitrogen Oxide emissions from nonsooty swirling flames of natural gas. Proc Combust Inst 1994; 25: 235-242.

[27] Smart JP, Weber R. Reduction of NOx and optimisation of burnout with an aerodynamically airstaged burner and an air staged pre-combustor burner. J Inst Energy 1989; 62: 237-245.

[28] Parham JJ, Nathan GJ, Smart JP, Hill SJ, Jenkins BG. The relationship between heat flux and NOx emissions in gas fired rotary kilns. J Inst Energy 2000; 73: 25-34.

[29] Weber R, Orsino S, Verlaan AL, Lallemant N. Combustion of light and heavy fuel oils in high-temperature air. J Inst of Energy 2001; 74: 38-47.

[30] Murphy JJ, Shaddix CR. Soot property measurements in a two-meter diameter JP-8 pool fire. Combust Sci Technol 2008; 178: 865-894.

[31] Kearney SP, Frederickson K, Grasser TW. Dual-pump coherent anti-Stokes Raman scattering thermometry in a sooting turbulent pool fire. Proc Combust Inst 2009; 32: 871-878.

[32] Antonia RA, Satyaprakash BR, Hussain AKMF. Measurements of dissipation rate and some other characteristics of turbulent plane and circular jets. Phys Fluids 1980; 23: 695-700.

[33] Decroix ME, Roberts WL. Transient flow field effects on soot volume fraction in diffusion flames. Comb Sci Tech 2000; 160: 165-189.

[34] Kent JH, Bastin SJ. Parametric effects on sooting in turbulent acetylene diffusion flames. Combust Flame 1984; 56: 29-42.

[35] Qamar NH, Nathan GJ, Alwahabi ZT, King KD. The effect of global mixing on soot volume fraction: measurements in simple jet, precessing jet, and bluff body flames. Proc Combust Inst 2005; 30: 1493-1500.

[36] Masri AR, Dibble RW, Barlow RS. The structure of turbulent non-

premixed flames revealed by Raman-Rayleigh-LIF measurements. Prog Energy Combust Sci 1996; 22: 307-362.

[37] Dally BB, Masri AR, Barlow RS, Fiechtner GJ. Instantaneous and mean compositional structure of bluff-body stabilised nonpremixed flames. Combust Flame 1998; 114: 119-148.

[38] Dugué J, Weber R, Horsman H. The effect of combustion on swirling flows expanding in a medium confinement furnace. IFRF Document No F 59/y/7. International Flame Research Foundation; 1990.

[39] Dugué J, Ereaut PR. Laser sheet visualisation in cold flows, gas and coal flames. IFRF Document No. K 70/y/241-12. International Flame Research Foundation; 1990.

[40] Frederickson K, Kearney SP, Grassner TW, Castaneda JN. Joint temperature and soot-volume-fraction measurements in turbulent meter-scale pool fires . In: 47th AIAA Aerospace Sciences Meeting. AIAA 2009-1264. Orlando, USA; 2009.

[41] Hoffman D, Leipertz A. Temperature field measurements in a sooting flame by filtered Rayleigh scattering (FRS). Proc Combust Inst 1996; 26: 945-950.

[42] Miles RB, Forkey JN, Lempert WR. Filtered Rayleigh scattering measurements in supersonic/hypersonic facilities. In: AIAA 17th Aerospace Ground Testing Conference, AIAA-92-3894, AIAA; Nashville, USA: 1992.

[43] Yalin AP, Miles RB. Ultraviolet filtered Rayleigh scattering temperature measurements with a mercury filter. Opt Lett 1999; 24: 590-592.

[44] Hoffman D, Münch KU, Leipertz A. Two-dimensional temperature determination in sooting flames by filtered Rayleigh scattering. Opt Lett 1996; 21: 525-527.

[45] Elliott GS, Glumac N, Carter CD. Molecular filtered Rayleigh scattering applied to combustion. Meas Sci Technol 2001; 12: 452-466.

[46] Kearney SP, Schefer RW, Beresh SJ, Grasser TW. Temperature imaging in nonpremixed flames by joint filtered Rayleigh and Raman scattering. Appl Opt 2005; 44: 1548-1558.

[47] Eckbreth AC. Laser Diagnostics for Combustion Temperature and Species. Gordon and Breach Publishers; Amsterdam: 1996.

[48] Meier W, Weigand P, Duan XR, Giezendanner-Thoben R. Detailed characterization of the dynamics of thermoacoustic pulsations in a lean premixed swirl flame. Combust Flame 2007; 150: 2-26.

[49] Afzelius M, Bengtsson PE, Bood J, Brackmann C, Kurtz A. Development of multipoint vibrational coherent anti-Stokes Raman spectroscopy for flame applications. Appl Opt 2006; 45: 1177-1186.

[50] Stricker W, Lückerath R, Meier U, Meier W. Temperature measurements in combustion - not only with CARS: a look back at one aspect of the European CARS Workshop. J Raman Spectrosc 2003; 34: 922-931.

[51] Roy S, Meyer TR, Lucht RP, Belovich VM, Corporan E, Gord JR. Temperature and CO_2 concentration measurements in the exhaust stream of a liquid-fuelled combustor using dual-pump coherent anti-Stokes Raman scattering (CARS) spectroscopy. Combust Flame 2004; 138: 273-284.

[52] Roy S, Kinnius PJ, Lucht RP, Gord JR. Temperature measurements in reacting flows by time-resolved femtosecond coherent anti-Stokes Raman scattering (fs-CARS) spectroscopy. Opt Commun 2008; 281: 319-325.

[53] Weikl MC, Seeger T, Wendler M, Sommer R, Beyrau F, Leipertz A. Validation experiments for spatially resolved one-dimensional emission spectroscopy temperature measurements by dual-pump CARS in a sooting flame. Proc Combust Inst 2009; 32: 745-752.

[54] Malarski A, Beyrau F, Leipertz A. Interference effects of C2-radicals in nitrogen vibrational CARS thermometry using a frequency-doubled Nd:YAG laser. J Raman Spectrosc 2005; 36: 102-108.

[55] Geigle KP, Schneider-Kühnle Y, Tsurikov MS, Hadef R, Lückerath R, Krüger R, Stricker W, Aigner M. Investigation of laminar pressurised flames for soot model validation using SV-CARS and LII. Proc Combust Inst 2005; 30: 1645-1653.

[56] Kliewer CJ, Gao Y, Seeger T, Kiefer J, Patterson BD, Setterson TB. Picosecond time-resolved pure-rotational coherent anti-StokesRaman spectroscopy in sooting flames. Proc Combust Inst 2010; 33: DOI: 10.1016/j.proci.2010.05.067.

[57] Hartlieb AT, Atakan B, Kohse-Höinghaus K. Temperature measurement in fuel-rich non-sooting low-pressure hydrocarbon flames. Appl Phys B 2000; 70: 435-445.

[58] Seitzman JM, Hanson RK, DeBarber PA, Hess CF. Application of quantitative two-line OH planar laser-induced fluorescence for temporally resolved planar thermometry in reacting flows. Appl Opt 1994; 33: 4000-4012.

[59] Cattolica R. OH rotational temperature from two-line laser-excited fluorescence. Appl Opt 1981; 20: 1156-1166.

[60] Giezendanner-Thobe R, Meier U, Meier W, Aigner M. Phase-locked temperature measurements by two-line OH PLIF thermometry of a self-excited combustion instability in a gas turbine model combustor. Flow Turbul Combust 2005; 75: 317-333.

[61] Qin W, Chen YL, Lewis JWL. Time-resolved temperature images of laser-ignition using OH two-line laser-induced fluorescence (LIF) thermometry, Tech. Rep. Article Number 200508, IFRF Combustion Journal: 2005.

[62] Nygren J, Engström J, Walewski J, Kaminski CF, Aldén M. Applications and evaluation of two-line atomic LIF thermometry in sooting combustion environments. Meas Sci Technol 2001; 12: 1294-1303.

[63] Haudiquert M, Cessou A, Stepowski D, Coppalle A. OH and soot measurements in a high-temperature laminar diffusion flame. Combust Flame 1997; 111: 338-349.

[64] Tamura M, Luque J, Harrington JE, Berg PA, Smith GP, Jeffries JB, Crosley DR. Appl Phys B 1998; 66: 503-510.

[65] Bessler WG, Hildenbrand F, Schulz C. Two-line laser-induced fluorescence imaging of vibrational temperatures of seeded NO. Appl Opt 2001; 40: 748-756.

[66] Kronemayer H, Ifeacho P, Hecht C, Dreier T, Wiggers H, Schulz C. Gas-temperature imaging in a low-pressure flame reactor for nano-particle synthesis with multi-line NO-LIF thermometry. Appl Phys B 2007; 88: 373-377.

[67] Lee T, Jeffries JB, Hanson RK. Experimental evaluation of strategies for quantitative laser-induced-fluorescence imaging of nitric oxide in high-pressure flames (1-60 bar). Proc Combust Inst 2007; 31: 757-764.

[68] Atakan B, Hartlieb AT. Laser diagnostics of NO reburning in fuel-rich propene flames. Appl Physics B 71 (2000) 697-702.

[69] McMillin BK, Palmer JL, Hanson RK. Temporally resolved, two-line fluorescence imaging of NO temperature in a transverse jet in a supersonic cross flow. Appl Opt 1993; 32: 7532-7545.

[70] Schulz C, Sick V. Tracer-LIF diagnostics: quantitative measurement of fuel concentration, temperature and fuel/air ratio in practical combustion systems. Prog Energy Combust Sci 2005; 31: 75-121.

[71] Hanson RK, Seitzman JM, Paul PH. Planar laser-fluorescence imaging of combustion gases. Appl Phys B 1990; 50: 441-454.

[72] Einecke S, Schulz C, Sick V. Measurement of temperature, fuel concentration and equivalence ratio fields using tracer LIF in IC engine combustion. Appl Phys B 2000; 71: 717-723.

[73] Luong M, Zhang R, Schulz C, Sick V. Toluene laser-induced fluorescence for in-cylinder temperature imaging in internal combustion engines. Appl Phys B 2008; 91: 669-675.

[74] Robinson GA, Lucht RP, Laurendeau NM. Two-color planar laser-induced fluorescence thermometry in aqueous solutions. Appl Opt 2008; 47: 2852-2858.

[75] Dabiri D. Digital particle image thermometry/velocimetry: a review. Exp Fluids 2009; 46: 191-241.

[76] Särner G, Richter M, Aldén M. Two-dimensional thermometry using temperature-induced line shifts of ZnO:Zn and ZnO:Ga fluorescence. Opt Lett 2008; 33: 1327-1329.

[77] Hirasawa T, Kamata Y, Kaneba T, Nakamura Y. Visualization of ambient gas temperature based on two-color LIF. In: 9th Asia-Pacific Conference on Combustion. Taipei, Taiwan; National Taiwan University: 2009.

[78] Medwell PR, Chan QN, Kalt PAM, Alwahabi ZT, Dally BB, Nathan GJ. Development of temperature imaging using two-line atomic fluorescence. Appl Opt 2009; 48: 1237-1248.

[79] Haraguchi H, Winefordner JD. Flame diagnostics: Local temperature

profiles and atomic fluorescence intensity profiles in air-acetylene flames. Appl Spectrosc 1977; 31: 195-200.

[80] Engström J, Nygren J, Aldén M, Kaminski CF. Two-line atomic fluorescence as a temperature probe for highly sooting flames. Opt Lett 2000; 25: 1469-1471.

[81] Aldén M, Grafström P, Lundberg H, Svanberg S. Spatially resolved temperature measurements in a flame using laser-excited two-line atomic fluorescence and diode-array detection. Opt Lett 1983; 8: 241-243.

[82] Joklik RG, Daily JW. Two-line atomic fluorescence temperature measurement in flames: an experimental study. Appl Opt 1982; 21: 4158-4162.

[83] Haraguchi H, Smith B, Weeks S, Johnson DJ, Winefordner JD. Measurement of small volume flame temperatures by the two-line atomic fluorescence method. Appl Spectrosc 1977; 31: 156-163.

[84] Kaminski CF, Engström J, Aldén M. Quasi-instantaneous two-dimensional temperature measurements in a spark ignition engine using 2-line atomic fluorescence. Proc Combust Inst 1998; 27: 85-93.

[85] Medwell PR, Chan QN, Kalt PAM, Alwahabi ZT, Dally BB, Nathan GJ. Instantaneous Temperature Imaging of Diffusion Flames Using Two-Line Atomic Fluorescence. Appl Spectrosc 2010; 64: 173-176.

[86] Chan QN, Medwell PR, Kalt PAM, Alwahabi ZT, Dally BB, Nathan GJ. Simultaneous Imaging of Temperature and Soot Volume Fraction. Proc Combust Inst 2010; 33: DOI 10.1016/j.proci.2010.06.031.

[87] Chan QN, Medwell PR, Kalt PAM, Alwahabi ZT, Dally BB, Nathan GJ. Solvent Effects on Two-Line Atomic Fluorescence (TLAF) of Indium. Applied Optics 2010; 49: 1257-1266.

[88] Chan QN, Medwell PR, Alwahabi ZT, Dally BB, Nathan GJ. Assessment of Interferences to Nonlinear Two-line Atomic Fluorescence (NT-LAF) in Sooty Flames Applied Physics B 2010; submitted.

[89] Klimenko AY. Multicomponent diffusion of various admixtures in turbulent flow. Fluid Dyn 1990; 25: 327-334.

[90] Peters N. Laminar flamelet concepts in turbulent combustion. Proc Combust Inst 1986; 21: 1231-1250.

[91] Bilger RW. Conditional moment closure for turbulent reacting flow. Phys Fluids A 1993; 5: 436-444.

[92] Hsu AG, Narayanaswamy V, Clemens NT, Frank JH. Mixture Fraction Imaging in turbulent non-premixed flames with two-photon LIF of krypton. Proc Combust Inst 2010; 33: DOI 10.1016/j.proci.2010.06.051.

[93] Chen YC, Starner SH, Masri AR. Characteristics of turbulent spray combustion in a piloted jet flame burner. Proc Combust Inst 2002; 29: 625-632.

[94] Masri AR, Kelman JB, Dally BB. The instantaneous spatial structure of the recirculation zone in bluff-body stabilised flames. Proc Combust Inst 1998; 27: 1031-1038.

[95] Barlow RS, Frank JH, Karpetis AN, Chen JY. Piloted methane/air jet flames: transport effects and aspects of scalar structure. Combust Flame 2005; 143: 433-449.

[96] Gregor MA, Seffrin F, Fuest F, Geyer D, Dreizler A. Multi-scalar measurements in a premixed swirl burner using 1D Raman/Rayleigh scattering. Proc Combust Inst 2009; 32: 1739-1746.

[97] Geyer D, Kempf A, Dreizler A, Janicka J. Turbulent opposed-jet flames: A critical benchmark experiment for combustion LES. Combust Flame 2005; 143: 524-548.

[98] Eckbreth AC. Effects of laser-modulated particulate incandescence on Raman scattering diagnostics. J Appl Phys 1977; 48: 4473-4479.

[99] Axelsson B, Collin R, Bengtsson PE. Laser-induced incandescence for soot particle size and volume measurements using on-line extinction calibration. Appl Phys B 2001; 72: 367-372.

[100] Appel J, Jungfleisch B, Marquardt M, Suntz R, Bockhorn H. Assessment of soot volume fractions from laser-induced incandescence by comparison with extinction measurements in laminar, premixed, flat flames. Proc Combust Inst 1996; 26: 2387-2395.

[101] Vanderwal RL, Zhou Z, Choi MY. Laser-induced incandescence calibration via gravimetric sampling. Combust Flame 1996; 105: 462-470.

[102] Bengtsson PE, Aldén M. Application of a pulsed laser for soot measurements in premixed flames. Appl Phys B 1989; 48: 155-164.

[103] Zerbs J, Geigle KP, Lammel O, Hader J,Stirn R, Hadef R, Meier W. The influence of wavelength in extinction measurements and beam steering in laser-induced incandescence measurements in sooting flames. Appl Phys B 2009; 96: 683694.

[104] Qamar NH, Alwahabi ZT, Chan QN, Nathan GJ, Roekaerts D, King KD. Soot volume fraction in a piloted turbulent jet non-premixed flame of natural gas. Combust Flame 2009; 156: 1339-1347.

[105] Henriksen TL, Nathan GJ, Alwahabi ZT, Qamar NH, Ring TA, Eddings EG. Planar measurements of soot volume fraction and OH in a JP-8 pool fire. Combust Flame 2009; 156: 1480-1492.

[106] Lee SY, Turns SR, Santoro R.J. Measurements of soot, OH, and PAH concentrations in turbulent ethylene/air jet flames. Combust Flame 2009; 156: 2264-2275.

[107] Alwahabi ZT, Qamar NH, Nathan GJ. unpublished results.

[108] Black DL, McQuay MQ, Bonin MP. Laser-based techniques for particle-size measurement: A review of sizing methods and their industrial applications. Prog Energy Combust Sci 1996; 22: 267-306.

[109] Kalt PAM, Nathan GJ, Kelso RM. Planar laser measurements of the aerodynamic agglomeration caused by Indigos Emitter. Report No. MECHTEST MT0659-3; School of Mechanical Engineering, University of Adelaide: 2005.

[110] Cassel HM, Liebman I. The cooperative mechanism in the ignition of dust dispersions. Combust Flame 1959; 3: 467-475.

[111] Dhodapkar S, Jacobs K, Hu S. In: Crowe CT, editor. Multiphase flow handbook: fluid-solid transport in ducts. Boca Raton, USA; CRC Press: 2005.

[112] Smith NL, Nathan GJ, Zhang DK, Nobes DS. The Significance of Particle Clusters in Pulverised Coal Flames. Proc Combust Inst 2002; 29: 797-804.

[113] Fan J, Zhao H, Cen K. An experimental study of two-phase turbulent coaxial jets. Exp Fluids 1992; 13: 279-287.

[114] Longmire EK, Eaton JK. Structure of a particle-laden round jet. J Fluid Mech 1992; 236: 217-257.

[115] Kalt PAM, Nathan GJ. Corrections to facilitate planar-imaging of particle concentration in particle-laden flow using Mie-scattering part 2: Diverging laser sheets Appl Opt 2007; 46: 7227-7236.

[116] Kalt PAM, Birzer CH, Nathan GJ. Corrections to facilitate planar imaging of particle concentration in particle-laden flows using Mie-scattering, part 1: Collimated laser sheets. Appl Opt 2007; 46: 5823-5834.

[117] Herzhaft B, Guazzelli E. Experimental study of the sedimentation of dilute and semi-dilute suspensions of fibres. J Fluid Mech 1999; 384: 133-158.

[118] Kuusela E, Lahtinen JM, Ala-Nissila T. Collective effects in settling of spheroids under steady-state sedimentation. Phys Rev Lett 2003; 90: 094502.

[119] Lin JZ, Shi X, Yu ZS. The motion of fibers in an evolving mixing layer. Int J Multiphase Flow 2003; 29: 1355-1372.

[120] Berrocal E, Kristensson E, Richter M, Linne MA, Aldén M. Application of structured illumination for multiple scattering suppression in planar laser imaging of dense sprays. Opt Express 2008; 16: 17870-17881.

[121] Kristensson E, Berrocal E, Richter M, Petterson SG, Aldén M. High-speed structured planar laser illumination for contrast improvement of two-phase flow images. Optics Letters 2008; 33: 2752-2754.

[122] Kalt PAM, Birzer CH, Nathan GJ. Quantified Nephelometry: Planar images of particle concentration in optically thick flows. In :Int. Conf. Multiphase Flows, 30 May - 4 June, Florida, USA: 2010.

Table 1: Typical operating conditions for industrial-scale flame and a $1/10^{th}$ scale model.

	d (m)	U (m/s)	d_p (µm)	L_F (m)
Reference	1	30	100	30
Model ($1/10^{\text{th}}$ scale)	0.1	See Table 2	100	3

Table 2: The influence on key dimensionless parameters of the choice of characteristic velocity (from Table 1), chosen for the model.

Scaling method	U_{model} (m/s)	$\frac{Re_{mod}}{Re_{full}}$	$\frac{U/S_{Lmod}}{U/S_{Lfull}}$	$\frac{\tau_{mod}}{\tau_{full}}$	$\frac{Sk_{mod}}{Sk_{full}}$
Const Re	300	$\times 1$	$\times 10$	$\times 0.01$	$\times 100$
Const U	30	$\times 0.1$	$\times 1$	$\times 0.1$	$\times 10$
Const τ	3	$\times 0.01$	$\times$ 0.1	$\times 1$	$\times 1$

List of Figures

1 The influence of physical scale on the NOx emissions from burners scaled using constant velocity scaling [25]. 65
2 Broadening of the Rayleigh line-shape as a function of temperature, in relation to the transmission of an iodine filter, as used for Filtered Rayleigh Scattering (FRS) thermometry [41]. 66
3 Two-dimensional image of temperature obtained using Filtered Rayleigh Scattering (top) and corresponding scattering image (bottom) collected without filtering [44]. 67
4 CARS excitation processes for nanosecond and femtosecond laser pulses [52]. 68
5 Instantaneous temperature images from two-line LIF of 3-pentanone in a two-stroke internal combustion engine. Black colouration indicates burned areas. Reproduced from Einecke *et al.* [72]. 69
6 Instantaneous planar measurement of temperature in the presence of soot, measured using Nonlinear excitation regime Two-Line Atomic Fluorescence (NTLAF), recorded simultaneously with soot volume fraction by Laser-Induced Incandescence (LII) in a wrinkled laminar flame. Reproduced from Chan *et al.* [86]. 70
7 Experimental arrangement for the simultaneous imaging of methane Raman scattering, Rayleigh scattering, and OH-LIF. 71
8 Experimental system for simultaneous line imaging of Raman scattering, Rayleigh scattering, and CO LIF [11] 72
9 Instantaneous image triplets of mixture fraction, temperature, and OH mass fraction collected in flame BB2 (90% of blow-off) [37]. Three triplets are presented for each axial location with images covering an 8-mm region centered at 22, 34, 46, and 62 mm. The flow is from bottom to top. Overlaid on the mixture fraction image are contours marking the lean (ξ=0.01, yellow) and rich (ξ=0.1, white) reactive limits of H_2/CH_4 fuel mixture. 73
10 A schematic diagram of the optical arrangement for the LII measurement. Reproduced from Qamar *et al.* [35]. 74
11 A photo of the flat flame produced a McKenna-style burner used for LII calibration 75

12 Schematic representation of the cylindrical (and potentially overlapping) shadows cast by spherical particles for the case of collimated light. Ray tracing can be used to correct for these attenuations [115, 116]. 76
13 The dependence of the intensity at each pixel in a diverging light sheet can be determined from its position in the light sheet by tracing back to the virtual origin [116]. 77
14 The simplified 1-D model of collimated attenuation used to correct for divergence by ray tracing from a planar image [116]. 78
15 The planar image of a spray generated by a laser sheet with a sinusoidal distribution of laser intensity, in turn imposed by the use of an optical grating [121]. 79
16 The difference between a raw planar image generated by a laser sheet through a spray (left) with that obtained using the SLIPI method to remove secondary scattering [121]. 80
17 Demonstration of simultaneous LII and PIV in a laminar diffusion flame. 81
18 The instantaneous planar measurement of all components of radiation propagation through a turbulent scattering, absorbing medium of spherical particles with a diverging light sheet [122]. 82

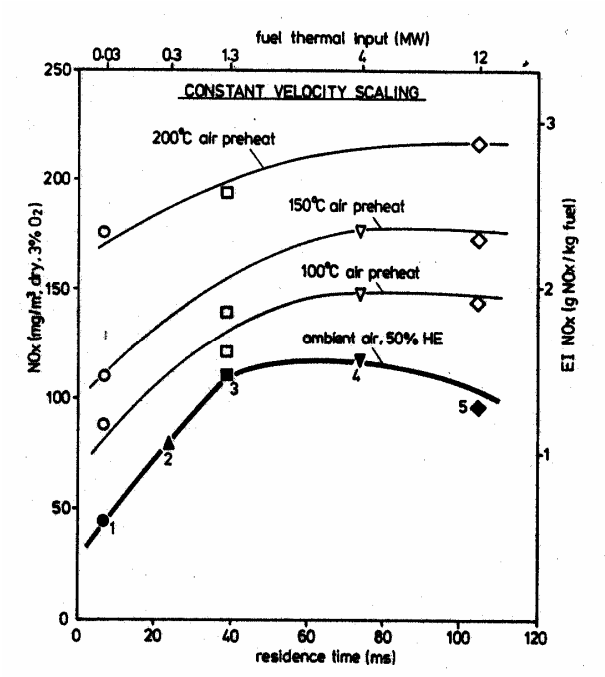

Figure 1: The influence of physical scale on the NOx emissions from burners scaled using constant velocity scaling [25].

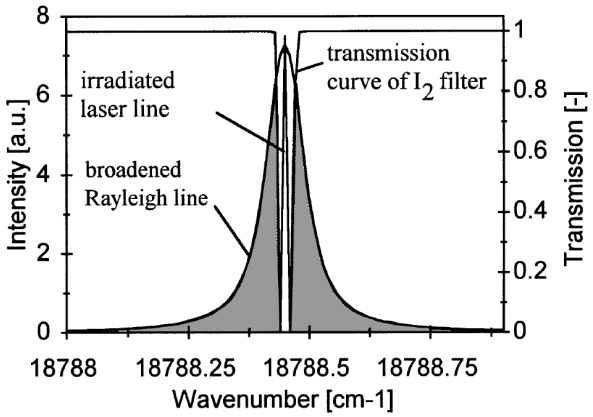

Figure 2: Broadening of the Rayleigh line-shape as a function of temperature, in relation to the transmission of an iodine filter, as used for Filtered Rayleigh Scattering (FRS) thermometry [41].

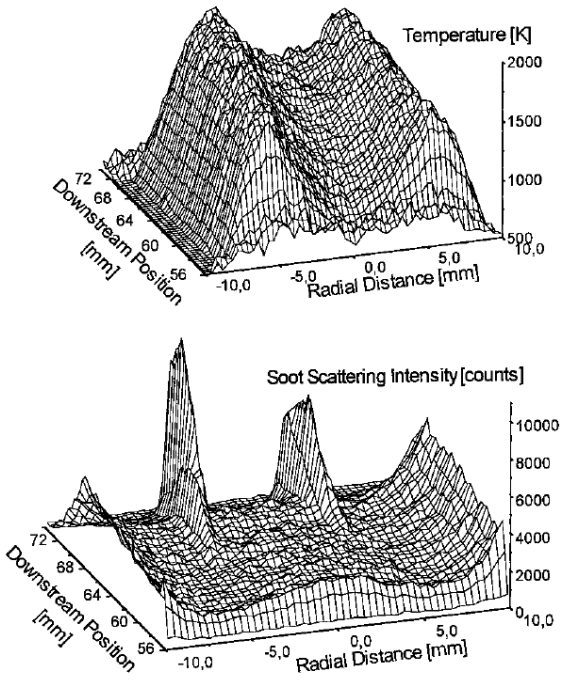

Figure 3: Two-dimensional image of temperature obtained using Filtered Rayleigh Scattering (top) and corresponding scattering image (bottom) collected without filtering [44].

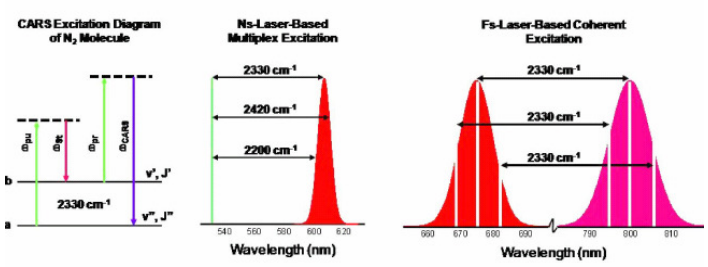

Figure 4: CARS excitation processes for nanosecond and femtosecond laser pulses [52].

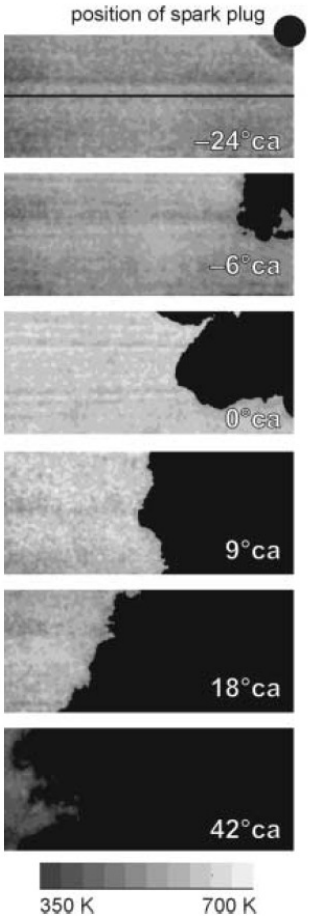

Figure 5: Instantaneous temperature images from two-line LIF of 3-pentanone in a two-stroke internal combustion engine. Black colouration indicates burned areas. Reproduced from Einecke *et al.* [72].

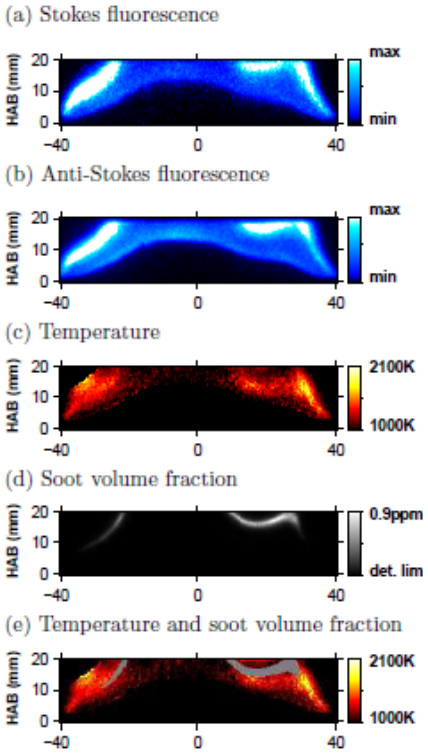

Figure 6: Instantaneous planar measurement of temperature in the presence of soot, measured using Nonlinear excitation regime Two-Line Atomic Fluorescence (NTLAF), recorded simultaneously with soot volume fraction by Laser-Induced Incandescence (LII) in a wrinkled laminar flame. Reproduced from Chan *et al.* [86].

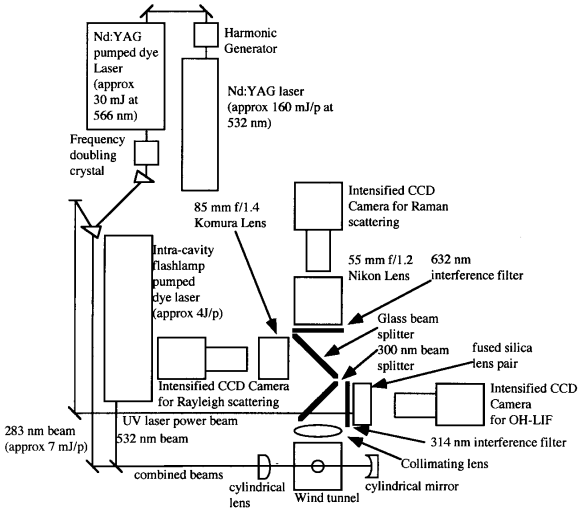

Figure 7: Experimental arrangement for the simultaneous imaging of methane Raman scattering, Rayleigh scattering, and OH-LIF.

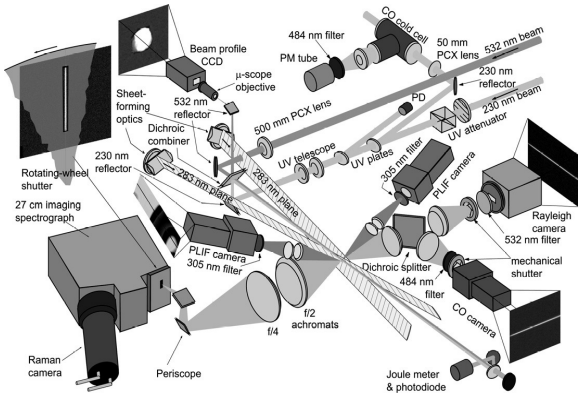

Figure 8: Experimental system for simultaneous line imaging of Raman scattering, Rayleigh scattering, and CO LIF [11]

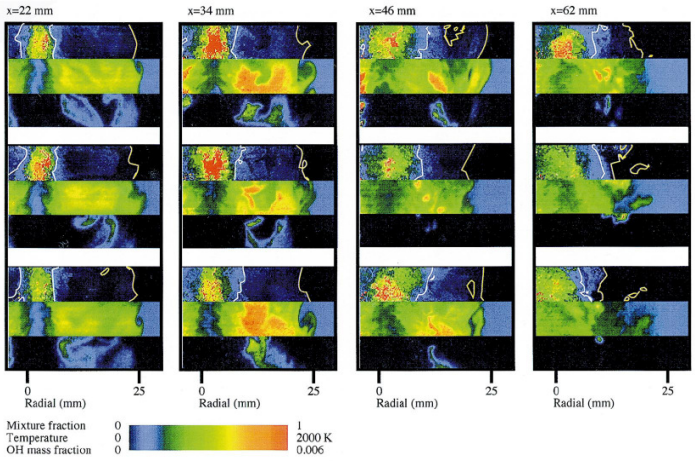

Figure 9: Instantaneous image triplets of mixture fraction, temperature, and OH mass fraction collected in flame BB2 (90% of blow-off) [37]. Three triplets are presented for each axial location with images covering an 8-mm region centered at 22, 34, 46, and 62 mm. The flow is from bottom to top. Overlaid on the mixture fraction image are contours marking the lean (ξ=0.01, yellow) and rich (ξ=0.1, white) reactive limits of H_2/CH_4 fuel mixture.

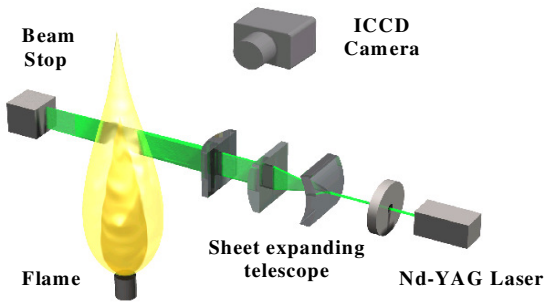

Figure 10: A schematic diagram of the optical arrangement for the LII measurement. Reproduced from Qamar *et al.* [35].

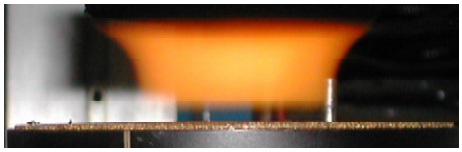

Figure 11: A photo of the flat flame produced a McKenna-style burner used for LII calibration

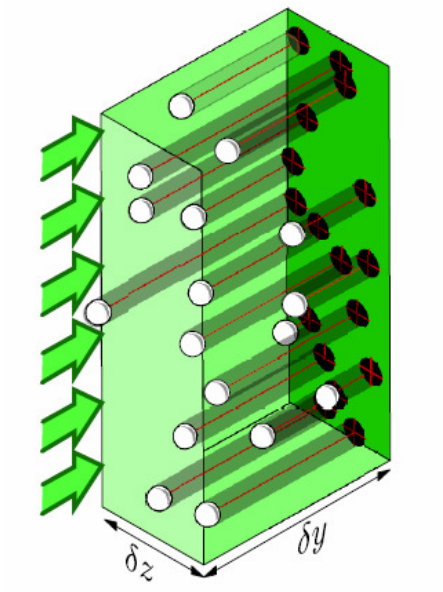

Figure 12: Schematic representation of the cylindrical (and potentially overlapping) shadows cast by spherical particles for the case of collimated light. Ray tracing can be used to correct for these attenuations [115, 116].

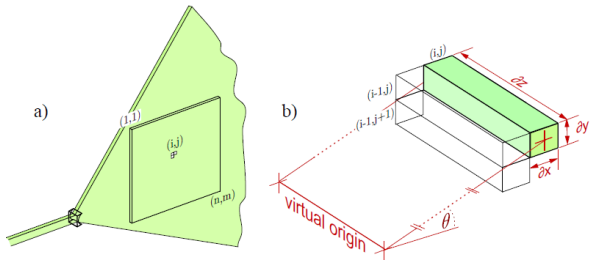

Figure 13: The dependence of the intensity at each pixel in a diverging light sheet can be determined from its position in the light sheet by tracing back to the virtual origin [116].

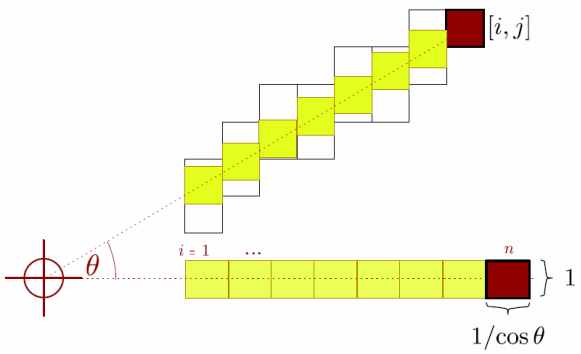

Figure 14: The simplified 1-D model of collimated attenuation used to correct for divergence by ray tracing from a planar image [116].

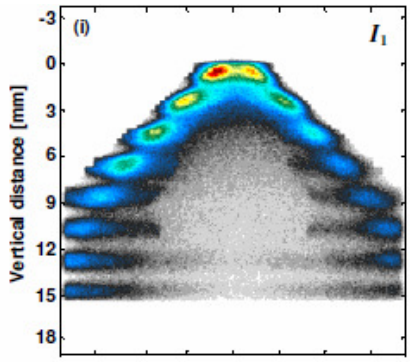

Figure 15: The planar image of a spray generated by a laser sheet with a sinusoidal distribution of laser intensity, in turn imposed by the use of an optical grating [121].

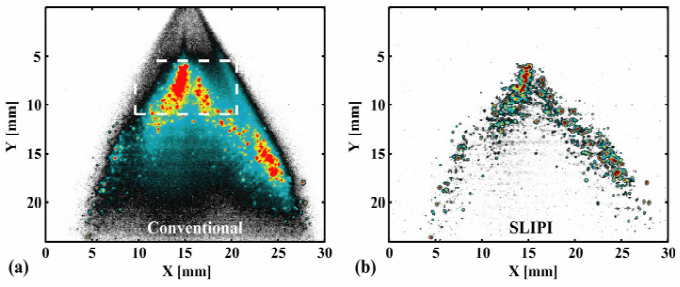

Figure 16: The difference between a raw planar image generated by a laser sheet through a spray (left) with that obtained using the SLIPI method to remove secondary scattering [121].

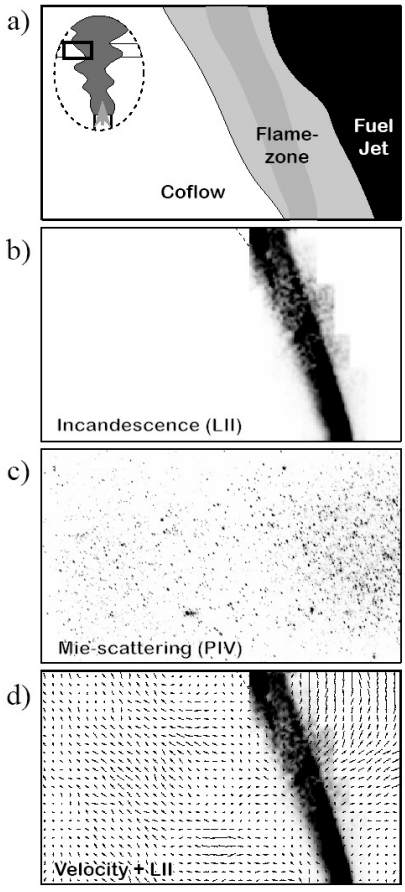

Figure 17: Demonstration of simultaneous LII and PIV in a laminar diffusion flame.

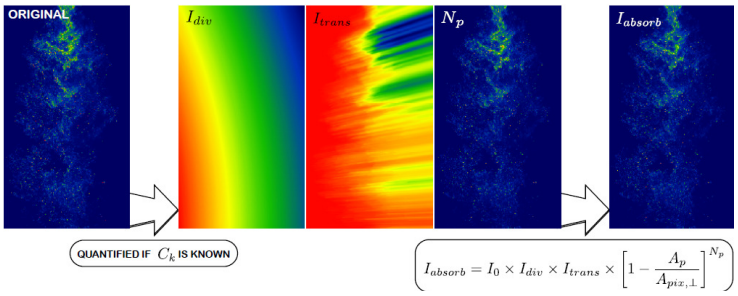

Figure 18: The instantaneous planar measurement of all components of radiation propagation through a turbulent scattering, absorbing medium of spherical particles with a diverging light sheet [122].